Elsevier Editorial System(tm) for Electrochimica Acta

Manuscript Draft

Manuscript Number: EO17-4120R1

Title: Electrochemistry and spectroelectrochemistry of polymers based on D-A-D and D-D-D bis(N-carbazolyl) monomers, effect of the donor/acceptor core on their properties

Article Type: Research Paper

Keywords: carbazole; phenothiazine; acridone; electroactive polymer; spectroelectrochemistry

Corresponding Author: Dr. Przemyslaw Data,

Corresponding Author's Institution: Durham University

First Author: Piotr Pander

Order of Authors: Piotr Pander; Agnieszka Swist, Dr; Pawel Zassowski; Jadwiga Soloducho, Prof.; Mieczyslaw Lapkowski, Prof.; Przemyslaw Data, Dr

Abstract: In this work we present electropolymerization of monomers of an unusual type using N-linked carbazole units to limit their conjugation. The polymers thus obtained have limited conjugation through the backbone. Using donor-acceptor-donor (D-A-D) and donor-donor-donor (D-D-D) monomers we evaluate the effects of the presence (or absence) of charge transfer states on synthesized electropolymers. The use of a D-A-D monomer resulted in obtaining an ambipolar polymer with quasi-reversible reduction.

***Response to Reviewers**

Reviewers' comments:

Reviewer #1: This is a nice paper which deserves publication. The synthetic part as well as the electrochemistry is sound and well done, and the new monomers are interesting.

On the other hand, the spectroscopic part is too short. What is the fluo QY of the monomers ? Do the polymer fluoresce (and in which state) ? A table gathering all this would be welcome. Even if a detailed paper on fluorescence is being written, though a couple of details would be welcome in the present article.

A table showing basic photophysical data (including Φ_{PL}) has been attached to the manuscript.

Polymers are not god emitters due to the fact that we cannot obtain fully undoped, purified polymers(oligomers), as the films are insoluble. We have only been able to observe luminescence from poly(2), however, as the paper is focused on electrochemistry, we decided not to include this observation here.

PLQY's shown in the work were measured in methylcyclohexane and all the spectroscopic part modified in order to adapt the changes. Cyclohexane and methylcyclohexane are very similar solvents so the results are in fact not affected by the change.

Please note that I do not comment on the ESR section, which is outside my expertise.

Reviewer #2: This manuscript by P. Data describes the electrochemistry and spectroelectrochemistry of two polymers. I think this paper can be reconsidered after addressing the following points:

1. Would the authors show practical applications of poly(1) and poly(2) as emitting layers in polymer light emitting diodes? I don't think that poly(2) is a promising emitting layer in polymer light emitting diodes. The carbonyl group in acridone unit serves as a fluorescence quenching unit.

*To make it more precise: we suggest only poly(2) to be used as OLED emitter, but not poly(1). Poly(1) and monomer 1 in general contain fluorescence-quenching phenoxazine that in fact eliminates the use of such a system as an emitter, however poly(2) and monomer 2 contain acridone that in fact is known as an efficient fluorescence emitter. Moreover, there are some examples of D-A-D molecules with acridone unit that show good PLQY. [*RSC Adv. 6 (2016) 17129–17137. doi:10.1039/C5RA25115J*] This is also confirmed in our work as monomer (2), containing acridone, has got high PLQY.*

We have observed that both polymers show zero or no emission when not fully undoped. We were able to observe greenish photoluminescence from poly(2) in an undoped form, however due to the fact that the polymer was not soluble in typical solvents such as DCM or chlorobenzene, chloroform, etc. a further (i.e. quantitive) purification was impossible. This is a typical drawback of electropolymerised films, so that quantitive removal of dopant is virtually impossible, thus they are not directly suitable as emitters. However, we do believe, a chemically-synthesized polymer(or in fact oligomer) should be soluble, thus easy to purify and will be much more luminescent, as the monomer is. We do encourage any groups willing to continue this work in that way.

2. Line 150, the shoulder of compound 1 does not locate at 350-400 nm.

Indeed, corrected to 350-420 nm.

3. Line 165. How about the shoulders of 1 and 2 in the emission spectra?

Values for emission blue edge added to the text.

4. The equation Eg-opt = <lambda>onset/1240 (eV) in Table 1 is wrong.

Corrected.

5. The authors should depict the solvent and salt for the electrochemical measurements of ferrocene/ferricinium (Fc/Fc+) redox couple.

Measurement is done in the same solvent and salt as all electrochemical measurements shown. A note was added to experimental section to clarify this.

6. The carbonyl group in acridone unit is an electron withdrawing group. The order of Eox-onset is poly(2) < poly(1) in Table 1 of current manuscript. The order of Eox-onset should be poly(1) < poly(2).

The difference may be due to a fraction of polymer (oligomer) in poly(2) being more conjugated, thus showing lower onset oxidation potential than poly(1).

7. The photographs of poly(1) and poly(2) at 0.3, 0.8 and 1.1 V in Figure 4 should be given.

It is true that photographs are good for visualization of strongly electrochromic polymers with high contrast values. However, we do think photographs will not give any scientific insight into the paper, thus are not necessary.

8. Figures 7 and 8, [vs] ---> [vs.].

Corrected.

Electrochemistry and spectroelectrochemistry of polymers based on D-A-D and D-D-D bis(*N*-carbazolyl) monomers, effect of the donor/acceptor core on their properties

P. Pander [a,b], A. Swist [d], P. Zassowski [a], J. Soloducho [d], M. Lapkowski [a,c], P. Data* [a,b,c,1]

[a] *Faculty of Chemistry, Silesian University of Technology, M. Strzody 9, 44-100 Gliwice, Poland*
[b] *University of Durham, Physics Department, South Road, Durham DH1 3LE, United Kingdom*
[c] *Center of Polymer and Carbon Materials, Polish Academy of Sciences, M. Curie-Sklodowskiej 34, 41-819 Zabrze, Poland*
[d] *Wroclaw University of Technology, Faculty of Chemistry, Wybrzeze Wyspianskiego 27, 50-370 Wroclaw, Poland*

E-mail: przemyslaw.data@durham.ac.uk

ABSTRACT

In this work we present electropolymerization of monomers of an unusual type using *N*-linked carbazole units to limit their conjugation. The polymers thus obtained have limited conjugation through the backbone. Using donor-acceptor-donor (D-A-D) and donor-donor-donor (D-D-D) monomers we evaluate the effects of the presence (or absence) of charge transfer states on synthesized electropolymers. The use of a D-A-D monomer resulted in obtaining an ambipolar polymer with *quasi*-reversible reduction.

[1]ISE member

KEYWORDS: carbazole; phenothiazine; acridone; electroactive polymer; spectroelectrochemistry

1 Introduction

Electroactive polymers are an already very well-examined group of materials with many interesting properties, that can be used as conductive and semiconductive layers, [1,2] polymer light emitting diode (PLED) emitters [3,4] and hosts, [5,6] electrochromic films [7-12] for the use in electrochromic windows, electrochemical capacitor materials, [13] controlled drug release systems, [14-16] membrane matrices, [17] electrostrictive materials, such as artificial muscles [18] and many more.

The area of conducting polymers has expanded greatly since the Nobel Prize for their discovery has been awarded. [19] Nowadays, several different groups of polymers are known, such as thiophene-, [20-24] chalcogenophene- [25-30] or carbazole-based, [31-35] among others, however there are still new systems to be investigated. An interesting field of study are branched polymers formed by electropolymerization of multifunctional monomers. Interestingly, these kind of molecular systems can be produced by the introduction of *N*-substituted carbazole side groups in monomers, such as in the systems investigated previously. [36] The connection of carbazole *via* nitrogen atom provides the weakest conjugation from all practical substitution positions of this unit. This was evaluated in certain studies and is especially important in designing molecular systems as thermally activated delayed fluorescence emitters. [37-41] However, the lack of conjugation between the polymerizable carbazole unit and the core can provide an interesting insight to the properties of both monomer and respective electropolymer. This is because, due to lack of conjugation, the polymerizable carbazole unit behaves independently from the core in the monomer,

therefore there will also be observed an independent behavior in the polymeric system produced.

Such kind of systems are presented in this work and examined from the (spectro)electrochemical and spectroscopic point of view. One system (**1**) consists of a phenothiazine core, that acts as a donor, with *N*-bonded carbazole units, therefore the compound has a donor-donor-donor (D-D-D) structure. The compound **2** has an acridone core that acts as an acceptor, and also *N*-bonded carbazoles as side groups, thus **2** has a donor-acceptor-donor (D-A-D) structure.

Scheme 1. Monomers studied in this work.

2 Experimental section

2.1 Materials.

All commercially available compounds were used as received. All solvents for the synthesis were dried and then distilled before use. Electrochemical measurements were performed in 10^{-3} M concentrations of all monomers for all voltammetric measurements (CV, DPV). Electrochemical studies were conducted in 0.1 M argon purged solutions of Bu_4NBF_4 (dried), 99% (Sigma-Aldrich) in dichloromethane (DCM), CHROMASOLV®, 99.9% (Sigma-Aldrich) and tetrahydrofuran (THF), 99.9%, Extra Dry, AcroSeal™ (ACROS Organics) solvents at room temperature. UV-Vis-NIR spectroelectrochemical measurements were performed on an Indium Tin Oxide (ITO) coated quartz working electrode. Polymeric layers were synthesized on an ITO electrode in conditions similar to that of cyclic voltammetric measurements.

2.1.1 *General synthesis.*

The synthetic procedure of 3,7-di(carbazol-9-yl)-*N*-butylphenothiazine (**1**), outlined at **Scheme 2**, was based on metal-catalyzed Ullmann-type C-N coupling reaction, efficient method to form novel carbon-nitrogen bond [42,43]. 3,7-Dibromo-*N*-butylphenothiazine, synthesized according to our previous experience [44], underwent nucleophilic aromatic substitution with carbazole, in a presence of a base and the copper-binding ligand 1,10-phenanthroline. An environment of the reaction were high-boiling polar solvent dimethylformamide and inert atmosphere.

The synthesis of 2,7-di(carbazol-9-yl)-*N*-hexylacridin-9-one (**2**), outlined in **Scheme 2**, was also based on copper-catalyzed condensation of 2,7-dibromo-*N*-hexylacridone with carbazole at the same conditions as stated above. 2,7-Dibromo-*N*-hexylacridone was synthesized according to a previously established procedure [45].

2.1.2 *3,7-di(carbazol-9-yl)-N-butylphenothiazine (**1**)*

3,7-Dibromo-*N*-butylphenothiazine (1.0 g, 2.42 mmol), carbazole (0.93g, 5.57 mmol) were placed in a three-necked flask with copper iodide (0.19 g, 1.02 mmol), potassium carbonate (1.51 g, 0.01 mol), 1,10-phenanthroline (0.36 g, 1.99 mmol) and 15 ml of *N*,*N*-dimethylformamide. The reaction mixture was heated at 145°C for 48h under a nitrogen atmosphere. Insoluble brown solid was filtered from the reaction mixture and washed with *ca*. 5 ml of *N*,*N*-dimethylformamide (product passed to a filtrate). Water was added to a filtrate and obtained solid was filtered and washed with water to remove copper compounds. A precipitate was purified by silica gel chromatography with hexane:ethyl acetate (9:1, V/V) as the eluent. 3,7-Di(carbazol-9-yl)-*N*-butylphenothiazine (**1**), grey-brown powder (mp >250°C), was obtained with 35% yield (0.50 g, 0.85 mmol).

^{1}H NMR (600 MHz, $CDCl_3$): 8.17 (d, *J*=7.7 Hz, 4H, arom. H), 7.47-7.39 (m, 12H, arom. H), 7.32 (t, *J*=6.8 Hz, 4H, arom. H), 7.15 (d, *J*=8.2 Hz, 2H, arom. H), 4.06 (s, 2H, N-CH_2) 2.02-

2.00 (m, 2H, CH_2), 1.66-1.62 (m, 2H, CH_2), 1.11 (t, *J*=7.4 Hz, 3H, CH_3). **^{13}C NMR (151 MHz, $CDCl_3$):** 144.3, 141.1, 132.5, 126.4, 126.2, 126.2, 126.0, 123.3, 120.3, 119.9, 116.2, 109.8, 47.7, 29.1, 20.4, 14.0. **MS m/z [%]** = 586.24.

*2.1.3 2,7-di(carbazol-9-yl)-N-hexylacridin-9-one (**2**)*

2,7-Dibromo-*N*-hexylacridin-9-one (1.0 g, 2.29 mmol), carbazole (0.88g, 5.26 mmol) were placed in a three-necked flask with copper iodide (0.24 g, 1.26 mmol), potassium carbonate (1.42 g, 0.01 mol), 1,10-phenanthroline (0.35 g, 1.94 mmol) and 15 ml of *N*,*N*-dimethylformamide. The reaction mixture was heated at 145°C for 22h under a nitrogen atmosphere. Insoluble grey-green solid was filtered from the reaction mixture and washed with dimethylformamide (product passed to a filtrate). Water was added to a filtrate and obtained solid was filtered and washed with water to remove copper compounds. Yellow-green precipitate was the product **2** 2,7-di(carbazol-9-yl)-*N*-hexylacridin-9-one (0.74 g, 1.21 mmol). The yield of the reaction – 53%, mp >250°C.

^{1}H NMR (600 MHz, $CDCl_3$): 8.87 (d, *J*=2.6 Hz, 2H, arom. H), 8.21 (d, *J*=7.7 Hz, 4H, arom. H), 8.02 (dd, *J*=9.1 Hz, *J*=2.6 Hz, 2H, arom. H), 7.84 (d, *J*=9.1 Hz, 2H, arom. H), 7.50 (d, *J*=8.1 Hz, 4H, arom. H), 7.46 (t, *J*=7.6 Hz, 4H, arom. H), 7.35 (t, *J*=7.4 Hz, 4H, arom. H), 4.57 (t, *J*=8.4 Hz, 2H, N-CH_2) 2.18-2.15 (m, 2H, CH_2), 1.73-1.70 (m, 2H, CH_2), 1.59-1.55 (m, 2H, CH_2), 1.51-1.49 (m, 2H, CH_2), 1.02 (t, *J*=6.9 Hz, 3H, CH_3). **^{13}C NMR (151 MHz, $CDCl_3$):** 176.9, 140.9, 140.6, 133.0, 131.7, 126.1, 125.9, 123.5, 123.4, 120.4, 120.2, 116.7, 109.6, 47.0, 31.6, 27.4, 26.7, 22.7, 14.1. **MS m/z [%]** = 610.29.

Scheme 2. Synthetic route used to obtain investigated monomers.

2.2 *Measurements.*

Melting points were determined on automatic melting point SMP10 (Stuart) apparatus. NMR spectra were taken in $CDCl_3$ by Avance 400 (Bruker) at 600 MHz for ^{1}H and ^{13}C at ambient temperature. Chemical shifts are reported in parts per million (δ) relative to tetramethylsilane (δ = 0.0 ppm). MS spectra were taken on a Bruker micrOTOF-Q, FWHM-17500, 20 Hz. The electrochemical investigation was carried out using Autolab PGSTAT20 and PGSTAT100 (Metrohm Autolab) potentiostats. The electrochemical cell comprised of a platinum disk with 1 mm diameter of working area as working electrode, Ag/AgCl electrode as a reference electrode and a platinum wire as an auxiliary electrode. The reference electrode was calibrated against ferrocene/ferrocenium redox couple in the same conditions (solvent, salt) as all electrochemical measurements. Cyclic voltammetry measurements were conducted at room temperature with scan rate of 50 mV s^{-1}. UV-Vis-NIR spectra in spectroelectrochemical analysis were recorded by QE6500 and NIRQuest detectors (Ocean Optics). Absorption and emission spectra of monomers were collected using a UV-3600 double beam spectrophotometer (Shimadzu), and a Fluorolog or Fluoromax-3 fluorescence spectrometer (Jobin Yvon). In situ EPR spectroelectrochemical experiments were performed using JES-FA 200 (JEOL) spectrometer. *g*-factor value has been determined with the aid of JEOL internal standard, knowing that the third line of the Mn-standard spectrum has a g-factor of 2.03324. The width of the EPR signal has been calculated as a distance in mT between minimum and maximum of the spectrum.

2.3 *Calculations*

DFT calculations of ground state geometry and MO surfaces have been carried out using the B3LYP hybrid functional combined with a 6-31G(d,p) basis set. For all investigated compounds ground state geometries were optimized. All calculations have been carried out with Jaguar [46] version 9.3 release 15 in Maestro Materials Science 2.3 in Maestro Materials

Suite 2016-3 software package. [47] Spin density of radicals was calculated using the same basis set and functional with spin set to 2 and charge set to +1 and -1 for radical cation and anion, respectively. All alkyl chains have been reduced to methyl groups to decrease calculation complexity.

3 Results and discussion

3.1 3.1 Photophysical investigation of monomers

Absorption spectrum (**Figure 1**) of **1** consists of a shoulder (λ = 350-420 nm) that can clearly be associated as n-π* transition involving the lone pairs of nitrogen and sulfur in the phenothiazine unit. The shoulder is followed by an absorption band at λ_{max} = 327, 339 nm which due to its characteristic shape should be associated with n-π* transition of carbazole. The next absorption band λ_{max} = 293 nm is also associated with carbazole. The compound due to very weak absorption at wavelengths > 380 nm gives colorless solutions. On the other hand, **2** shows a well defined CT band with λ_{max} = 409 nm. In systems like **1** or **2**, due to the lack of conjugation between the carbazole and core it is possible to observe the absorption bands of all moieties separately. In this case neither carbazole [48] nor acridone [49] absorb in the region of >410 nm, therefore the new band can be attributed to CT. The absorption band that in **2** is at λ_{max} = 323 nm seems to be present in all acridone derivatives substituted at 2,7 position by donors [49]. This band seems to shift with the type of donor attached and is not present in **1**, therefore such absorption originates from acridone. This band however overlaps with the n-π* band of carbazole which is therefore barely observable. Similarly to **1**, in **2** the π-π* absorption band of carbazole λ_{max} = 293 nm is observed. Emission of the molecules in solution is blue with maximum at 436 nm and 442 nm and blue edge at 400 nm and 412 nm respectively for **1** and **2**.

Calculated HOMO and LUMO orbital surfaces (**Figure S1**, **S2**) confirm the experimental observations . In **1** the HOMO→LUMO transition shows a local n-π* character, but in **2** the HOMO→LUMO transition has a hybrid local and charge transfer (HLCT) character. This however explains a relatively strong absorption of this band in comparison to π-π* bands as HOMO/LUMO overlap is significant.

Table 1. Basic photophysical properties of investigated monomers.

Figure 1. a) UV-Vis and fluorescence spectra of monomers in methylcyclohexane solution. b) DPV voltammograms of investigated compounds recorded in DCM and THF solutions of Bu_4NBF_4 supporting electrolyte.

3.2 Electrochemical investigation of monomers and electropolymerization

The monomers show clearly different electrochemical properties both in terms of oxidation and reduction (**Figure 2,3**). **1** due to the D-D-D structure undergoes only oxidation, no reduction was observed within the electrochemical potential window. The oxidation comprises two reversible signals that can be attributed to the first and second oxidation steps of phenothiazine. The first oxidation process clearly leads to formation of a stable radical cation located at phenothiazine (see EPR section). Second redox couple should therefore be associated with the formation of a dication. The following oxidation processes can be associated with oxidation of carbazole moieties. This reaction is irreversible and leads to formation of a conductive polymer. The compound **2** oxidizes solely at the carbazole moieties, which results in formation of a polymer, similarly to **1**. This compound however, due to the D-A-D structure, also undergoes reduction. A reduction peak (see **Figure 2**) can be observed within the electrochemical window, moreover the process is reversible. Further

investigation of the reduction process by EPR spectroscopy confirms the formation of a stable radical anion located at the acridone moiety in this case. Carbazole moieties in **2** oxidize at lower potential than in **1**, but **1** contains an electron-rich and **2** bears electron-deficient core. This happens due to the fact that oxidation of carbazoles in **1** undergoes with the bicationic ($\mathbf{1}^{2+}$) instead of the neutral form. Such a bication is repulsed from the working electrode surface at positive potential applied, moreover the phenothiazine bication core acts now as an electron-deficient unit. Both effects draw the oxidation potential of carbazole units in **1** to higher values.

As observed with DPV (**Figure 2**) at positive potentials, oxidation of **1** over 1 V potential is complicated, comprising many overlapping peaks. These are the signals of electropolymerization overlapped with the electrochemical response of the forming polymer. On the other hand oxidation of **2** is well resolved, comprising two clearly visible peaks. The first peak has to be associated with the monoelectron oxidation of a single carbazole moiety of **2**, the second process is probably associated with electrochemical response of the forming polymer due to its broadened shape. It is worth to note that the oxidation peak of **2** recorded with CV technique is stretched and deformed, this is because it actually consists of two signals mentioned above (as seen by DPV), that are overlapped.

Figure 2. a), b) Cyclic voltammograms of monomers showing first oxidation / reduction cycles. c), d) Cyclic voltammograms showing electropolymerization process in consecutive scans (black line); Stability of the polymer recorded in monomer-free solution (red line). Oxidation recorded in DCM, reduction in THF solutions of Bu_4NBF_4 supporting electrolyte. Scan rate 0.05 V s^{-1}.

As mentioned previously, the two monomers electropolymerize well, forming a stable polymeric film (see **Figure 3**). The electropolymerization process is induced by the presence of carbazole moieties, that after monoelectron oxidation undergo a coupling reaction. Although carbazole appears to be a bifunctional monomer, recent works [50,51] suggest carbazole acting as a monofunctional moiety in the molecular systems comprising two or more *N*-carbazolyl species. This also seems to be true in the monomers presented here and is supported by (spectro)electrochemical data. In example, the polymers do not increase their conjugation length as presented in the voltammograms – oxidation *onset* remains unchanged in following polymerization scans. Both polymers show electrochemical responses similar to the already reported cases. [52] The first oxidation process of the polymers has to be attributed to formation of polarons, whereas the second to bipolaronic species, which is further confirmed by spectroelectrochemistry.

Figure 3. Cyclic voltammograms of poly(**2**) recorded in DCM and THF solutions of Bu_4NBF_4 supporting electrolyte. Scan rate 0.05 V s^{-1}.

Following the reasoning given above, the proposed polymer structure of poly(**1**) and poly(**2**) is shown in **Scheme 3**. It becomes clear that the acridone/phenothiazine bridge units break the conjugation between bicarbazole bridges, resulting in formation of a polymer with short conjugation length. Please also see **Figure S3-S6**. The calculations performed on idealized trimers show that although there is some conjugation between the bicarbazoles and cores, the units are clearly out of plane. Polymers inherit some features of the monomers, such as redox or optical properties. In particular, the polymer of a D-D-D monomer consequently does not reduce, moreover, the neutral film is colorless, similarly to the solution of the monomer. On the other hand, poly(**2**) color is similar to the yellow color of monomer's solution, due to the presence of a similar charge transfer band, absorbing blue light. Poly(**2**) also shows a

reduction process of *quasi*-reversible character at the potential similar to the redox pair of the monomer (see **Figure 4**). Clearly, the reduction of the polymer involves the acridone species as in both cases: the monomer and polymer the reduction occurs at almost the same potential, -2.07 V and -2.15 V, respectively (see **Table 2**). In this case, due to limited diffusion rate of counter ions the anodic and cathodic peak are stretched and deformed. EPR investigation of the polymer reveals hardly no signal upon reduction of the polymer. This suggests a somehow regular, stacked structure of the polymer, allowing the radical anions of acridone to stack, forming i.e. spinless dimers, which is similar to the already reported dimers in ethylenedioxythiophene-based systems. [9,53]

Scheme 3. Proposed structure of electrodeposited polymers studied in this work.

At this point it is important to note the coincidence of electrochemical and optical energy gap of **2** and poly(**2**). The values are very close in both cases suggesting electron binding energy of zero or almost zero. In this case an error of ± 0.03 eV to the values can be assumed. This is still a debate whether forbidden transition such as n-π* or CT can be used to determine energy gap of a molecule as respective absorption band may not be visible in the spectrum. The answer to this question is not definite, in some cases a forbidden transition has relatively large oscillator strength, thus being well defined in the absorption spectrum. If that condition is met, as in **2** and poly(**2**), the optical energy gap can be determined properly with a small error.

Table 2. Electrochemical properties of investigated molecules.

3.3 UV-Vis-NIR spectroelectrochemical investigation of monomers and polymers

To fully understand the electrochromic response of polymers it is necessary to study the oxidation of monomers first (**Figure 5**). In case of **1** the most interesting part is the oxidation of phenothiazine moiety leading to the formation of a monocation (cation radical) and, at higher potential applied, a bication. Both these species are seen in the absorption spectra. Interestingly, the absorption of a phenothiazine cation radical is very specific and clearly is not present in the spectra of oxidized polymer. Oxidation of **2** leads to formation of a polymer which is a result of coupling of cation radicals originating from carbazole moieties. Due to the similarity of monomer's and polymer's cation radical structure the spectra observed resemble the electrochromic response of poly(**2**).

Figure 4. a), b) UV-Vis-NIR spectroelectrochemical analysis of electrochemical oxidation of **1** and **2**; c), d) Electrochromic response of respective polymers. P1, P2 denote first and second polaronic band; BP bipolaronic band; N neutral polymer absorption bands. Spectra recorded in DCM / 0.1 mol dm^{-3} Bu_4NBF_4 supporting electrolyte solution using ITO coated quartz working electrode.

Electrochromic response of polymers is similar to the already reported [52] cases. Two polaronic bands (P1, P2) are arising in the first oxidation step and one bipolaronic (BP) arises above a specific potential in the second oxidation step. The potentials at which formation of polarons/bipolarons is observed are in good correlation with the *onset* potential of the first and second oxidation peak of polymers, respectively. Therefore figures determining *onset* potential of formation of bipolarons allow to attribute the first redox reaction in polymers to the neutral ↔ polaronic redox process. The second redox process should consequently be attributed to the polaronic ↔ bipolaronic redox process. In both cases oxidation of the polymeric film shows diminishing absorption of the neutral polymer absorption bands (N). This is due to oxidation of bis(carbazolyl) bridges that connect mers. Interestingly, in both

cases there is an isosbestic point clearly visible between N and P1 bands. As no shift of that point is observed, this indicates perfect reversibility of the doping/dedoping process between neutral and polaronic forms. Additional isosbestic point can be observed between P1 and BP bands in poly(**2**). This is rather associated with the presence of a CT band in the polymer, which is discussed below. The presence of an isosbestic point here suggests the process of bipolarons formation to be connected with the diminish of the CT band.

Poly(**2**) similarly to the monomer shows a charge transfer transition. The charge transfer appears clearly between the non-conjugated units of acridone (acceptor) and bicarbazole bridges (donor). Interestingly, the first polaronic band (P1) of the polymer is overlapped with the CT absorption band of a neutral film. The polaronic band grows on the top of the CT band and both bands are still overlapped at the potential of 0.60 V. Above that potential, along with the formation of bipolarons, the CT band diminishes. The band maximum shifts giving eventually absorbtion spectrum which is much more similar to the respective spectrum of poly(**1**) which does not have a CT. That means the polymer in a bipolaronic state shows no CT due to the lack of electrons at HOMO (as for neutral form), so HOMO→LUMO transition (CT) is suppressed.

What is even more interesting is that the electrochromic response of poly(**1**) does not clearly show the involvement of radical cations nor bications of phenothiazine. The polymer behaves on one hand very similar to poly(**2**) showing similar polaronic and bipolaronic bands – on the other hand, due to the absence of the CT band, the film is colorless. Thin films of poly(**1**) are not visible to human eye, but they become visible upon oxidation. This behavior is potentially interesting for applications such as electrochromic tinted windows. Electrochromic response of the polymer is however interesting as no observable evidence for the formation of normal phenothiazine radical cation / bication is present in the absorption spectra. This is further discussed in the ESR spectroelectrochemistry section.

3.4 ESR spectroelectrochemical investigation of monomers and polymers

To evaluate the origin of radical anion/cation species formed in the reversible redox processes the EPR technique has been used. The results comply with intuitive expectations, that reduction of **2** involves the acridone moiety, forming a radical anion, whereas the first oxidation step of **1** leads to production of radical cations localized at the phenothiazine moiety. The EPR spectrum of **2** radical anion shows hyperfine coupling constants of α_{1H} = 0.390 mT (2H) and α_{2H} = 0.365 mT (2H). The observed signal correlates with the simulated spin density for the anion radical (**Figure 6**). Radical is situated the most on atoms of C=O group which also stabilizes the negative charge due to its electron-defficient nature. The observed coupling constants are however only due to delocalization of the spin density over the π-conjugated carbon backbone, no coupling with nitrogen atom (^{14}N, S = 1) is observed as spin density at this atom is negligible. Long range coupling with neighboring atoms is not observed due to a small value of respective coupling constants.

Figure 5. Electron spin resonance (ESR) spectra of investigated cation radicals, linewidth 0.1 mT; hyperfine coupling constants (mT) attributed to the position of coupled nucleus (insets). Hyperfine constants determining coupling with protons are shown at the position of a respective proton, whereas hydrogen atoms themselves are not shown.

On the other hand the **1** radical cation has a spectrum showing hyperfine constants of α_{1N} = 0.749 mT (1N) and α_{1H} = 0.384 mT (2H). This is consistent with the simulated radical spin density (**Figure 6**). The radical is delocalized over the π-conjugated backbone, but the nitrogen and sulfur atoms also contribute to the structure. Coupling constants with nitrogen atoms of carbazolyl units are not observed due to their small values.

Figure 6. Spin density at the B3LYP/6-31G(d,p)/PBF(DCM) for investigated radicals. Isovalue is equal to 0.003.

The polymers however show a rather typical behavior for carbazole polymers, nevertheless this is not an expected behavior when their structure is considered (see **Figure 7**, **8**). Both polymers show no EPR signal in the neutral state suggesting no polaronic species are trapped or remain in defects / at the chain ends. The polymers show a rapid increase of EPR signal intensity upon film oxidation indicating the formation of polaronic species. The response of the polymers is perfectly reversible in the potential window shown. Upon expansion of the potential range to higher potential values the response becomes no longer perfectly reversible as, due to formation of bipolaronic species and long experiment times, the film undergoes slow degradation. The results shown here are therefore limited to the potential range where polymers show fine stability. Signal width decrease along with the decrease of the giromagnetic factor (*g*-factor) observed is an indication of formation of polarons. When the relative spin concentration increases, both factors stabilize their values indicating formation of a narrow variety of polaronic states. This shows that polymers have a regular structure and is consistent with the proposed polymer structure (**Scheme 3**) as the radicals formed localize mostly at bicarbazole bridges in the polymer. Application of a potential of 0.7-0.9 V to the polymer films results in formation of bipolarons. This can be observed as a decrease or plateau of spin concentration. When the polaron concentration reaches a high level the existing or newly formed polarons become further oxidized to bipolarons. The formation of bipolarons is also often connected with slight broadening of the EPR signal that can be observed at higher potentials in poly(**2**) film.

Figure 7. ESR spectroelectrochemical analysis of poly(**1**). a) selected spectra; b) relative spin concentration vs. potential applied; c) signal width vs. potential applied; d) *g*-factor vs. potential applied. A cyclic voltamogram of the polymer film recorded at 0.01 V s^{-1} scan speed prior to the measurement is shown in figures b), c), d). Linewidth 0.05 mT.

The only question that arises in the interpretation of the polymers' behavior is why it is that similar. In case of poly(**1**) normally it would be expected that formation of radical cations occurs not only at bicarbazoles but also at phenothiazine units. The radicals observed in polymers show a g-factor of g = 2.0034-2.0035, which is much lower than the value for cation radical formed by **1**, which is g = 2.0052. If the formation of such phenothiazine-localized radical cations was a fact, there would be observed a large (or at least any) change of the g-factor during the potential sweep (i.e. oxidation of phenothiazine preceding oxidation of bicarbazoles or *vice versa*), however, this does not happen. Moreover, the EPR signal clearly indicates a presence of only one type of radical species (**Figure S7**). Interestingly, the signal of phenothiazine redox couple has not been observed in electrochemistry nor UV-Vis-NIR spectroelectrochemistry. Explanation of this fact is that the geometry of the polymer, especially at oxidized state, allows the phenothiazine to be conjugated with the carbazole moiety. In this situation the formation of a radical coupled with a nitrogen atom ("normal" phenothiazine radical cation) is thus inhibited. As such radical cations are not formed, their characteristical absorption bands cannot be observed in UV-Vis-NIR spectroelectrochemistry of poly(**1**).

Figure 8. ESR spectroelectrochemical analysis of poly(**2**). a) selected spectra; b) relative spin concentration vs. potential applied; c) signal width vs. potential applied; d) *g*-factor vs. potential applied. A cyclic voltamogram of the polymer film recorded at 0.01 V s^{-1} scan speed prior to the measurement is shown in figures b), c), d). Linewidth 0.04 mT.

Due to the conjugation between bicarbazoles and phenothiazine another kind of radical cation and bication species is likely to be formed. Also see Figure **S3**, **S4**. Such as polarons involve only the carbon atoms of phenothiazine, thus chromophoric nitrogen atom of this unit does not play a role. Very similar behavior has already been reported in 2,7-linked chalcogenophene-carbazole polymers [54].

4 Conclusions

Two novel monomers with *N*-linked carbazole species and D-D-D or D-A-D structure are presented. Both polymerize well, giving stable films. Poly(**1**) has shown particularly interesting behavior, giving no electrochemical, nor spectroelectrochemical evidence for formation of phenothiazine-based radical cations nor bications. Such behavior is a result of conjugation between bicarbazole bridges and phenothiazine in the oxidated state resulting in one oxidized form to be produced, rather than two (bicarbazole, phenothiazine) separately. It was observed that poly(**2**) – D-A-D based polymer shows a CT absorption band, similarly to the monomer. Interestingly, the band is present in the polaronic form of the polymer, while disappears in the bipolaronic form.

Transparency and colorlessness of poly(**1**) gives a promising potential application of the polymer in i.e. electrochromic tinted windows, while ambipolarity of poly(**2**) is promising in a potential application as an emitting layer in polymer light emitting diodes.

Acknowledgments

This work is financially supported by Polish National Science Centre, Project No. 2012/05/B/ST5/00745. P. Data acknowledges award no. 04/040/RGJ17/0052 from the Rector of the Silesian University of Technology for research and development achievements.

References

[1] J.H. Cook, H.A. Al-Attar, A.P. Monkman, Effect of PEDOT-PSS resistivity and work function on PLED performance, Org. Electron. 15 (2014) 245–250. doi:10.1016/j.orgel.2013.11.029.

[2] L. Groenendaal, F. Jonas, D. Freitag, H. Pielartzik, J.R. Reynolds, Poly(3,4-ethylenedioxythiophene) and Its Derivatives: Past, Present, and Future, Adv. Mater. 12 (2000) 481–494. doi:10.1002/(SICI)1521-4095(200004)12:7<481::AID-ADMA481>3.0.CO;2-C.

[3] S. Burns, J. MacLeod, T. Trang Do, P. Sonar, S.D. Yambem, Effect of thermal annealing Super Yellow emissive layer on efficiency of OLEDs, Sci. Rep. 7 (2017) 40805. doi:10.1038/srep40805.

[4] J. Santos, J.H. Cook, H.A. Al-Attar, A.P. Monkman, M.R. Bryce, Fluorene co-polymers with high efficiency deep-blue electroluminescence, J. Mater. Chem. C. 3 (2015) 2479–2483. doi:10.1039/c4tc02766c.

[5] V. Jankus, K. Abdullah, G.C. Griffiths, H. Al-Attar, Y. Zheng, M.R. Bryce, A.P. Monkman, The role of exciplex states in phosphorescent OLEDs with poly(vinylcarbazole) (PVK) host, Org. Electron. Physics, Mater. Appl. 20 (2015) 97–102. doi:10.1016/j.orgel.2015.02.002.

[6] H.A. Al Attar, A.P. Monkman, Dopant effect on the charge injection, transport, and device efficiency of an electrophosphorescent polymeric light-emitting device, Adv. Funct. Mater. 16 (2006) 2231–2242. doi:10.1002/adfm.200600035.

[7] P. Data, P. Pander, M. Lapkowski, A. Swist, J. Soloducho, R.R. Reghu, J. V. Grazulevicius, Unusual properties of electropolymerized 2,7- and 3,6- carbazole derivatives, Electrochim. Acta. 128 (2014) 430–438. doi:10.1016/j.electacta.2013.12.108.

[8] P. Data, P. Pander, P. Zassowski, V. Mimaite, K. Karon, M. Lapkowski, J.V. Grazulevicius, P. Slepski, K. Darowicki, Electrochemically Induced Synthesis of Triphenylamine-based Polyhydrazones, Electrochim. Acta. 230 (2017) 10–21. doi:10.1016/j.electacta.2017.01.132.

[9] P. Pander, P. Data, R. Turczyn, M. Lapkowski, A. Swist, J. Soloducho, A.P. Monkman, Synthesis and characterization of chalcogenophene-based monomers with pyridine acceptor unit, Electrochim. Acta. 210 (2016) 773–782. doi:10.1016/j.electacta.2016.05.185.

[10] A. Patra, Y.H. Wijsboom, S.S. Zade, M. Li, Y. Sheynin, G. Leitus, M. Bendikov, Poly(3,4-ethylenedioxyselenophene), J. Am. Chem. Soc. 130(21) (2008) 6734–6736. doi:10.1021/ja8018675.

[11] W. Yang, J. Zhao, C. Cui, Y. Kong, P. Li, Characterization and Electrochemical Synthesize from Selenophene-Substituted Poly(Triphenylamine) as Anodically Materials for Electrochromic Devices, Int. J. Electrochem. Sci. 7 (2012) 7960-7975.

[12] P. Data, R. Motyka, M. Lapkowski, J. Suwinski, A.P. Monkman, Spectroelectrochemical Analysis of Charge Carriers as a Way of Improving Poly(p-phenylene)-Based Electrochromic Windows, J. Phys. Chem. C. 119 (2015) 20188–20200. doi:10.1021/acs.jpcc.5b06846.

[13] T. V Vernitskaya, O.N. Efimov, Polypyrrole: a conducting polymer; its synthesis, properties and applications, Russ. Chem. Rev. 66 (1997) 443–457. doi:10.1070/RC1997v066n05ABEH000261.

[14] B. Alshammary, F.C. Walsh, P. Herrasti, C. Ponce de Leon, Electrodeposited conductive polymers for controlled drug release: polypyrrole, J. Solid State Electrochem. 20 (2016) 839–859. doi:10.1007/s10008-015-2982-9.

[15] K. Krukiewicz, M. Cichy, P. Ruszkowski, R. Turczyn, T. Jarosz, J.K. Zak, M. Lapkowski, B. Bednarczyk-Cwynar, Betulin-loaded PEDOT films for regional chemotherapy, Mater. Sci. Eng. C. 73 (2017) 611–615. doi:10.1016/j.msec.2016.12.115.

[16] D. Svirskis, J. Travas-Sejdic, A. Rodgers, S. Garg, Electrochemically controlled drug delivery based on intrinsically conducting polymers, J. Control. Release. 146 (2010) 6–15. doi:10.1016/j.jconrel.2010.03.023.

[17] A. Stolarczyk, W. Domagala, R. Turczyn, A. Januszkiewicz – Kaleniak, K. Kempska, K. Krukiewicz, M. Gnus, M. Lapkowski, The influence of oxygen conditioning effect on the permeation properties of polyaniline membranes, Sep. Sci. Technol. 6395 (2016) 1–8. doi:10.1080/01496395.2016.1171241.

[18] T. Mirfakhrai, J.D.W. Madden, R.H. Baughman, Polymer artificial muscles, Mater. Today. 10 (2007) 30–38. doi:10.1016/S1369-7021(07)70048-2.

[19] https://www.nobelprize.org/nobel_prizes/chemistry/laureates/2000/advanced-chemistryprize2000.pdf [accessed 24.04.2017]

[20] U. Mehmood, A. Al-Ahmed, I.A. Hussein, Review on recent advances in polythiophene based photovoltaic devices, Renew. Sustain. Energy Rev. 57 (2016) 550–561. doi:10.1016/j.rser.2015.12.177.

[21] T. Yamamoto, Molecular assembly and properties of polythiophenes, NPG Asia Mater. 2 (2010) 54–60. doi:10.1038/asiamat.2010.37.

[22] P. Data, P. Zassowski, M. Lapkowski, W. Domagala, S. Krompiec, T. Flak, M. Penkala, A. Swist, J. Soloducho, W. Danikiewicz, Electrochemical and spectroelectrochemical comparison of alternated monomers and their copolymers based on carbazole and thiophene derivatives, Electrochim. Acta. 122 (2014) 118–129. doi:10.1016/j.electacta.2013.11.167.

[23] P. Ledwon, S. Pluczyk, K.R. Idzik, R. Beckert, M. Lapkowski, Bipolar properties of polythiophene derivatives with 1,3,5-triazineunits, Electrochim. Acta. 109 (2013) 395–402. doi:10.1016/j.electacta.2013.07.171.

[24] P. Zassowski, S. Golba, L. Skorka, G. Szafraniec-Gorol, M. Matussek, D. Zych, W. Danikiewicz, S. Krompiec, M. Lapkowski, A. Slodek, W. Domagala, Spectroelectrochemistry of alternating ambipolar copolymers of 4,4′- and 2,2′-bipyridine isomers and quaterthiophene, Electrochim. Acta. 231 (2017). doi:http://dx.doi.org/10.1016/j.electacta.2017.01.076.

[25] A. Patra, M. Bendikov, Polyselenophenes, J. Mater. Chem. 20 (2010) 422–433. doi:10.1039/B908983G.

[26] A.A. Jahnke, D.S. Seferos, Polytellurophenes, Macromol. Rapid Commun. 32 (2011) 943–951. doi:10.1002/marc.201100151.

[27] J. Razzell-Hollis, F. Fleischli, A.A. Jahnke, N. Stingelin, D.S. Seferos, J.-S. Kim, Effects of Side-Chain Length and Shape on Polytellurophene Molecular Order and Blend Morphology, J. Phys. Chem. C. 121 (2017) 2088–2098. doi:10.1021/acs.jpcc.6b11675.

[28] A. Patra, V. Agrawal, R. Bhargav, Shahjad, D. Bhardwaj, S. Chand, Y. Sheynin, M. Bendikov, Metal Free Conducting PEDOS, PEDOT, and Their Analogues via an

Unusual Bromine-Catalyzed Polymerization, Macromolecules. 48 (2015) 8760–8764. doi:10.1021/acs.macromol.5b01777.

[29] M. Lapkowski, R. Motyka, J. Suwinski, P. Data, Photoluminescent polytellurophene derivatives of conjugated polymers as a new perspective for molecular electronics, Macromol. Chem. Phys. 213 (2012) 29–35. doi:10.1002/macp.201100384.

[30] P. Data, M. Lapkowski, R. Motyka, J. Suwinski, Electrochemistry and spectroelectrochemistry of a novel selenophene-based monomer, Electrochim. Acta. 59 (2012) 567–572. doi:10.1016/j.electacta.2011.11.021.

[31] M. Ates, N. Uludag, Carbazole derivative synthesis and their electropolymerization, J. Solid State Electrochem. 20 (2016) 2599–2612. doi:10.1007/s10008-016-3269-5.

[32] K. Karon, M. Lapkowski, A. Dabuliene, A. Tomkeviciene, N. Kostiv, J. V. Grazulevicius, Spectroelectrochemical characterization of conducting polymers from star-shaped carbazole-triphenylamine compounds, Electrochim. Acta. 154 (2015) 119–127. doi:10.1016/j.electacta.2014.12.092.

[33] R.R. Reghu, D. Volyniuk, N. Kostiv, K. Norvaisa, J. V. Grazulevicius, Symmetry versus asymmetry: Synthesis and studies of benzotriindole-derived carbazoles displaying different electrochemical and optical properties, Dye. Pigment. 125 (2016) 159–168. doi:10.1016/j.dyepig.2015.10.013.

[34] K. Laba, P. Data, P. Zassowski, K. Karon, M. Lapkowski, P. Wagner, D.L. Officer, G.G. Wallace, Electrochemically induced synthesis of poly(2,6-carbazole), Macromol. Rapid Commun. 36 (2015) 1749–1755. doi:10.1002/marc.201500260.

[35] I. Lévesque, P.-O. Bertrand, N. Blouin, M. Leclerc, S. Zecchin, G. Zotti, C.I. Ratcliffe, D.D. Klug, X. Gao, F. Gao, J.S. Tse, Synthesis and Thermoelectric Properties of Polycarbazole, Polyindolocarbazole, and Polydiindolocarbazole Derivatives, Chem. Mater. 19 (2007) 2128–2138. doi:10.1021/cm070063h.

[36] A. Palma-Cando, U. Scherf, Electrochemically Generated Thin Films of Microporous Polymer Networks: Synthesis, Properties, and Applications, Macromol. Chem. Phys. 217 (2016) 827–841. doi:10.1002/macp.201500484.

[37] F.B. Dias, K.N. Bourdakos, V. Jankus, K.C. Moss, K.T. Kamtekar, V. Bhalla, J. Santos, M.R. Bryce, A.P. Monkman, Triplet harvesting with 100% efficiency by way of thermally activated delayed fluorescence in charge transfer OLED emitters, Adv. Mater. 25 (2013) 3707–3714. doi:10.1002/adma.201300753.

[38] P. Data, P. Pander, M. Okazaki, Y. Takeda, S. Minakata, A.P. Monkman, Dibenzo[a,j]phenazine-Cored Donor-Acceptor-Donor Compounds as Green-to-Red/NIR Thermally Activated Delayed Fluorescence Organic Light Emitters, Angew. Chemie - Int. Ed. 55 (2016) 5739–5744. doi:10.1002/anie.201600113.

[39] H. Uoyama, K. Goushi, K. Shizu, H. Nomura, C. Adachi, Highly efficient organic light-emitting diodes from delayed fluorescence., Nature. 492 (2012) 234–8. doi:10.1038/nature11687.

[40] L. Mei, J. Hu, X. Cao, F. Wang, C. Zheng, Y. Tao, X. Zhang, W. Huang, The inductive-effect of electron withdrawing trifluoromethyl for thermally activated delayed fluorescence: tunable emission from tetra- to penta-carbazole in solution processed blue OLEDs., Chem. Commun. 51 (2015) 13024–7. doi:10.1039/c5cc04126k.

[41] F.B. Dias, T.J. Penfold, A.P. Monkman, Photophysics of thermally activated delayed fluorescence molecules, Methods Appl. Fluoresc. 5 (2017) 12001. doi:10.1088/2050-6120/aa537e.

[42] Z. Xi, F. Liu, Y. Zhou, W. Chen, CuI/L (L=pyridine-functionalized 1,3-diketones) catalyzed C-N coupling reactions of aryl halides with NH-containing heterocycles, Tetrahedron 64 (2008) 4254-4259.

[43] H.-S. Kim, E.-S. Yu, Y.-H. Kim, J.-H. Kim, Compound for organic photoelectric device and organic photoelectric device including the same, US 2012/0305900 A1.

[44] J. Doskocz, J. Soloducho, J. Cabaj, M. Lapkowski, S. Golba, K. Palewska, Development in synthesis, electrochemistry, LB moieties of phenothiazine based units, Electroanalysis 19 (2007) 1394-1401.

[45] A. Swist, J. Cabaj, J. Soloducho, P. Data, M. Lapkowski, Novel acridone-based branched blocks as highly fluorescent materials, Synth. Met. 180 (2013) 1-8. doi: 10.1016/j.synthmet.2013.07.020.

[46] A.D. Bochevarov, E. Harder, T.F. Hughes, J.R. Greenwood, D.A. Braden, D.M. Philipp, D. Rinaldo, M.D. Halls, J. Zhang, R.A. Friesner, Jaguar: A high-performance quantum chemistry software program with strengths in life and materials sciences, Int. J. Quantum Chem. 113 (2013) 2110–2142. doi:10.1002/qua.24481.

[47] Materials Science Suite 2016-3, Schrödinger, LLC, New York, NY, 2016.

[48] M.C. Castex, C. Olivero, G. Pichler, D. Adès, A. Siove, Fluorescence, room temperature phosphorescence and photodegradation of carbazole compounds in

irradiated poly(methyl methacrylate) matrices, Synth. Met. 156 (2006) 699–704. doi:10.1016/j.synthmet.2006.03.015.

[49] B.K. Sharma, A.M. Shaikh, N. Agarwal, R.M. Kamble, Synthesis, photophysical and electrochemical studies of acridone-amine based donor–acceptors for hole transport materials, RSC Adv. 6 (2016) 17129–17137. doi:10.1039/C5RA25115J.

[50] K. Karon, M. Lapkowski, G. Juozas, Electrochemical and UV-Vis/ESR spectroelectrochemical properties of polymers obtained from isomeric 2,7- and 3,6-linked carbazole trimers; Influence of the linking topology on polymers properties, Electrochim. Acta. 123 (2014) 176–182. doi:10.1016/j.electacta.2013.12.180.

[51] M. Lapkowski, J. Zak, K. Karon, B. Marciniec, W. Prukala, The mixed carbon-nitrogen conjugation in the carbazole based polymer; The electrochemical, UVVis, EPR, and IR studies on 1,4 bis[(E)2-(9H-carbazol-9-yl) vinyl]benzene, Electrochim. Acta. 56 (2011) 4105–4111. doi:10.1016/j.electacta.2011.01.114.

[52] A. Brzeczek, P. Ledwon, P. Data, P. Zassowski, S. Golba, K. Walczak, M. Lapkowski, Synthesis and properties of 1,3,5-tricarbazolylbenzenes with star-shaped architecture, Dye. Pigment. 113 (2015) 640–648. doi:10.1016/j.dyepig.2014.09.033.

[53] P. Data, A. Swist, M. Lapkowski, J. Soloducho, K. Darowicki, A.P. Monkman, Evidence for Solid State Electrochemical Degradation Within a Small Molecule OLED, Electrochim. Acta. 184 (2015) 86–93. doi:10.1016/j.electacta.2015.10.047.

[54] P. Pander, R. Motyka, P. Zassowski, M. Lapkowski, A. Swist, P. Data, Electrochromic Properties of Novel Selenophene and Tellurophene Derivatives Based on Carbazole and Triphenylamine Core, J. Phys. Chem. C, Article ASAP, doi: 10.1021/acs.jpcc.7b00216.

[55] C.M. Cardona, W. Li, A.E. Kaifer, D. Stockdale, G.C. Bazan, Electrochemical considerations for determining absolute frontier orbital energy levels of conjugated polymers for solar cell applications, Adv. Mater. 23 (2011) 2367–2371. doi:10.1002/adma.201004554.

[56] J.-L. Bredas, Mind the gap!, Mater. Horiz. 1 (2014) 17–19. doi:10.1039/C3MH00098B.

Electrochemistry and spectroelectrochemistry of polymers based on D-A-D and D-D-D bis(*N*-carbazolyl) monomers, effect of the donor/acceptor core on their properties

P. Pander [a,b], A. Swist [d], P. Zassowski [a], J. Soloducho [d], M. Lapkowski [a,c], P. Data* [a,b,c,1]

[a] *Faculty of Chemistry, Silesian University of Technology, M. Strzody 9, 44-100 Gliwice, Poland*

[b] *University of Durham, Physics Department, South Road, Durham DH1 3LE, United Kingdom*

[c] *Center of Polymer and Carbon Materials, Polish Academy of Sciences, M. Curie-Sklodowskiej 34, 41-819 Zabrze, Poland*

[d] *Wroclaw University of Technology, Faculty of Chemistry, Wybrzeze Wyspianskiego 27, 50-370 Wroclaw, Poland*

E-mail: przemyslaw.data@durham.ac.uk

ABSTRACT

In this work we present electropolymerization of monomers of an unusual type using *N*-linked carbazole units to limit their conjugation. The polymers thus obtained have limited conjugation through the backbone. Using donor-acceptor-donor (D-A-D) and donor-donor-donor (D-D-D) monomers we evaluate the effects of the presence (or absence) of charge transfer states on synthesized electropolymers. The use of a D-A-D monomer resulted in obtaining an ambipolar polymer with *quasi*-reversible reduction.

[1]ISE member

KEYWORDS: carbazole; phenothiazine; acridone; electroactive polymer; spectroelectrochemistry

1 Introduction

Electroactive polymers are an already very well-examined group of materials with many interesting properties, that can be used as conductive and semiconductive layers, [1,2] polymer light emitting diode (PLED) emitters [3,4] and hosts, [5,6] electrochromic films [7-12] for the use in electrochromic windows, electrochemical capacitor materials, [13] controlled drug release systems, [14-16] membrane matrices, [17] electrostrictive materials, such as artificial muscles [18] and many more.

The area of conducting polymers has expanded greatly since the Nobel Prize for their discovery has been awarded. [19] Nowadays, several different groups of polymers are known, such as thiophene-, [20-24] chalcogenophene- [25-30] or carbazole-based, [31-35] among others, however there are still new systems to be investigated. An interesting field of study are branched polymers formed by electropolymerization of multifunctional monomers. Interestingly, these kind of molecular systems can be produced by the introduction of *N*-substituted carbazole side groups in monomers, such as in the systems investigated previously. [36] The connection of carbazole *via* nitrogen atom provides the weakest conjugation from all practical substitution positions of this unit. This was evaluated in certain studies and is especially important in designing molecular systems as thermally activated delayed fluorescence emitters. [37-41] However, the lack of conjugation between the polymerizable carbazole unit and the core can provide an interesting insight to the properties of both monomer and respective electropolymer. This is because, due to lack of conjugation, the polymerizable carbazole unit behaves independently from the core in the monomer,

therefore there will also be observed an independent behavior in the polymeric system produced.

Such kind of systems are presented in this work and examined from the (spectro)electrochemical and spectroscopic point of view. One system (**1**) consists of a phenothiazine core, that acts as a donor, with *N*-bonded carbazole units, therefore the compound has a donor-donor-donor (D-D-D) structure. The compound **2** has an acridone core that acts as an acceptor, and also *N*-bonded carbazoles as side groups, thus **2** has a donor-acceptor-donor (D-A-D) structure.

Scheme 1. Monomers studied in this work.

2 Experimental section

2.1 Materials.

All commercially available compounds were used as received. All solvents for the synthesis were dried and then distilled before use. Electrochemical measurements were performed in 10^{-3} M concentrations of all monomers for all voltammetric measurements (CV, DPV). Electrochemical studies were conducted in 0.1 M argon purged solutions of Bu_4NBF_4 (dried), 99% (Sigma-Aldrich) in dichloromethane (DCM), CHROMASOLV®, 99.9% (Sigma-Aldrich) and tetrahydrofuran (THF), 99.9%, Extra Dry, AcroSeal™ (ACROS Organics) solvents at room temperature. UV-Vis-NIR spectroelectrochemical measurements were performed on an Indium Tin Oxide (ITO) coated quartz working electrode. Polymeric layers were synthesized on an ITO electrode in conditions similar to that of cyclic voltammetric measurements.

2.1.1 *General synthesis.*

The synthetic procedure of 3,7-di(carbazol-9-yl)-*N*-butylphenothiazine (**1**), outlined at **Scheme 2**, was based on metal-catalyzed Ullmann-type C-N coupling reaction, efficient method to form novel carbon-nitrogen bond [42,43]. 3,7-Dibromo-*N*-butylphenothiazine, synthesized according to our previous experience [44], underwent nucleophilic aromatic substitution with carbazole, in a presence of a base and the copper-binding ligand 1,10-phenanthroline. An environment of the reaction were high-boiling polar solvent dimethylformamide and inert atmosphere.

The synthesis of 2,7-di(carbazol-9-yl)-*N*-hexylacridin-9-one (**2**), outlined in **Scheme 2**, was also based on copper-catalyzed condensation of 2,7-dibromo-*N*-hexylacridone with carbazole at the same conditions as stated above. 2,7-Dibromo-*N*-hexylacridone was synthesized according to a previously established procedure [45].

2.1.2 *3,7-di(carbazol-9-yl)-N-butylphenothiazine (**1**)*

3,7-Dibromo-*N*-butylphenothiazine (1.0 g, 2.42 mmol), carbazole (0.93g, 5.57 mmol) were placed in a three-necked flask with copper iodide (0.19 g, 1.02 mmol), potassium carbonate (1.51 g, 0.01 mol), 1,10-phenanthroline (0.36 g, 1.99 mmol) and 15 ml of *N*,*N*-dimethylformamide. The reaction mixture was heated at 145°C for 48h under a nitrogen atmosphere. Insoluble brown solid was filtered from the reaction mixture and washed with *ca*. 5 ml of *N*,*N*-dimethylformamide (product passed to a filtrate). Water was added to a filtrate and obtained solid was filtered and washed with water to remove copper compounds. A precipitate was purified by silica gel chromatography with hexane:ethyl acetate (9:1, V/V) as the eluent. 3,7-Di(carbazol-9-yl)-*N*-butylphenothiazine (**1**), grey-brown powder (mp >250°C), was obtained with 35% yield (0.50 g, 0.85 mmol).

^{1}H NMR (600 MHz, $CDCl_3$): 8.17 (d, *J*=7.7 Hz, 4H, arom. H), 7.47-7.39 (m, 12H, arom. H), 7.32 (t, *J*=6.8 Hz, 4H, arom. H), 7.15 (d, *J*=8.2 Hz, 2H, arom. H), 4.06 (s, 2H, N-CH_2) 2.02-

2.00 (m, 2H, CH_2), 1.66-1.62 (m, 2H, CH_2), 1.11 (t, *J*=7.4 Hz, 3H, CH_3). **^{13}C NMR (151 MHz, $CDCl_3$):** 144.3, 141.1, 132.5, 126.4, 126.2, 126.2, 126.0, 123.3, 120.3, 119.9, 116.2, 109.8, 47.7, 29.1, 20.4, 14.0. **MS m/z [%]** = 586.24.

*2.1.3 2,7-di(carbazol-9-yl)-N-hexylacridin-9-one (**2**)*

2,7-Dibromo-*N*-hexylacridin-9-one (1.0 g, 2.29 mmol), carbazole (0.88g, 5.26 mmol) were placed in a three-necked flask with copper iodide (0.24 g, 1.26 mmol), potassium carbonate (1.42 g, 0.01 mol), 1,10-phenanthroline (0.35 g, 1.94 mmol) and 15 ml of *N*,*N*-dimethylformamide. The reaction mixture was heated at 145°C for 22h under a nitrogen atmosphere. Insoluble grey-green solid was filtered from the reaction mixture and washed with dimethylformamide (product passed to a filtrate). Water was added to a filtrate and obtained solid was filtered and washed with water to remove copper compounds. Yellow-green precipitate was the product **2** 2,7-di(carbazol-9-yl)-*N*-hexylacridin-9-one (0.74 g, 1.21 mmol). The yield of the reaction – 53%, mp >250°C.

^{1}H NMR (600 MHz, $CDCl_3$): 8.87 (d, *J*=2.6 Hz, 2H, arom. H), 8.21 (d, *J*=7.7 Hz, 4H, arom. H), 8.02 (dd, *J*=9.1 Hz, *J*=2.6 Hz, 2H, arom. H), 7.84 (d, *J*=9.1 Hz, 2H, arom. H), 7.50 (d, *J*=8.1 Hz, 4H, arom. H), 7.46 (t, *J*=7.6 Hz, 4H, arom. H), 7.35 (t, *J*=7.4 Hz, 4H, arom. H), 4.57 (t, *J*=8.4 Hz, 2H, N-CH_2) 2.18-2.15 (m, 2H, CH_2), 1.73-1.70 (m, 2H, CH_2), 1.59-1.55 (m, 2H, CH_2), 1.51-1.49 (m, 2H, CH_2), 1.02 (t, *J*=6.9 Hz, 3H, CH_3). **^{13}C NMR (151 MHz, $CDCl_3$):** 176.9, 140.9, 140.6, 133.0, 131.7, 126.1, 125.9, 123.5, 123.4, 120.4, 120.2, 116.7, 109.6, 47.0, 31.6, 27.4, 26.7, 22.7, 14.1. **MS m/z [%]** = 610.29.

Scheme 2. Synthetic route used to obtain investigated monomers.

2.2 *Measurements.*

Melting points were determined on automatic melting point SMP10 (Stuart) apparatus. NMR spectra were taken in $CDCl_3$ by Avance 400 (Bruker) at 600 MHz for ^{1}H and ^{13}C at ambient temperature. Chemical shifts are reported in parts per million (δ) relative to tetramethylsilane (δ = 0.0 ppm). MS spectra were taken on a Bruker micrOTOF-Q, FWHM-17500, 20 Hz. The electrochemical investigation was carried out using Autolab PGSTAT20 and PGSTAT100 (Metrohm Autolab) potentiostats. The electrochemical cell comprised of a platinum disk with 1 mm diameter of working area as working electrode, Ag/AgCl electrode as a reference electrode and a platinum wire as an auxiliary electrode. The reference electrode was calibrated against ferrocene/ferrocenium redox couple in the same conditions (solvent, salt) as all electrochemical measurements. Cyclic voltammetry measurements were conducted at room temperature with scan rate of 50 mV s^{-1}. UV-Vis-NIR spectra in spectroelectrochemical analysis were recorded by QE6500 and NIRQuest detectors (Ocean Optics). Absorption and emission spectra of monomers were collected using a UV-3600 double beam spectrophotometer (Shimadzu), and a Fluorolog or Fluoromax-3 fluorescence spectrometer (Jobin Yvon). In situ EPR spectroelectrochemical experiments were performed using JES-FA 200 (JEOL) spectrometer. *g*-factor value has been determined with the aid of JEOL internal standard, knowing that the third line of the Mn-standard spectrum has a g-factor of 2.03324. The width of the EPR signal has been calculated as a distance in mT between minimum and maximum of the spectrum.

2.3 *Calculations*

DFT calculations of ground state geometry and MO surfaces have been carried out using the B3LYP hybrid functional combined with a 6-31G(d,p) basis set. For all investigated compounds ground state geometries were optimized. All calculations have been carried out with Jaguar [46] version 9.3 release 15 in Maestro Materials Science 2.3 in Maestro Materials

Suite 2016-3 software package. [47] Spin density of radicals was calculated using the same basis set and functional with spin set to 2 and charge set to +1 and -1 for radical cation and anion, respectively. All alkyl chains have been reduced to methyl groups to decrease calculation complexity.

3 Results and discussion

3.1 3.1 Photophysical investigation of monomers

Absorption spectrum (**Figure 1**) of **1** consists of a shoulder (λ = 350-420 nm) that can clearly be associated as n-π^* transition involving the lone pairs of nitrogen and sulfur in the phenothiazine unit. The shoulder is followed by an absorption band at λ_{max} = 327, 339 nm which due to its characteristic shape should be associated with n-π^* transition of carbazole. The next absorption band λ_{max} = 293 nm is also associated with carbazole. The compound due to very weak absorption at wavelengths > 380 nm gives colorless solutions. On the other hand, **2** shows a well defined CT band with λ_{max} = 409 nm. In systems like **1** or **2**, due to the lack of conjugation between the carbazole and core it is possible to observe the absorption bands of all moieties separately. In this case neither carbazole [48] nor acridone [49] absorb in the region of >410 nm, therefore the new band can be attributed to CT. The absorption band that in **2** is at λ_{max} = 323 nm seems to be present in all acridone derivatives substituted at 2,7 position by donors [49]. This band seems to shift with the type of donor attached and is not present in **1**, therefore such absorption originates from acridone. This band however overlaps with the n-π^* band of carbazole which is therefore barely observable. Similarly to **1**, in **2** the π-π^* absorption band of carbazole λ_{max} = 293 nm is observed. Emission of the molecules in solution is blue with maximum at 436 nm and 442 nm and blue edge at 400 nm and 412 nm respectively for **1** and **2**.

Calculated HOMO and LUMO orbital surfaces (**Figure S1**, **S2**) confirm the experimental observations . In **1** the HOMO→LUMO transition shows a local n-π* character, but in **2** the HOMO→LUMO transition has a hybrid local and charge transfer (HLCT) character. This however explains a relatively strong absorption of this band in comparison to π-π* bands as HOMO/LUMO overlap is significant.

Table 1. Basic photophysical properties of investigated monomers.

Figure 1. a) UV-Vis and fluorescence spectra of monomers in methylcyclohexane solution. b) DPV voltammograms of investigated compounds recorded in DCM and THF solutions of Bu_4NBF_4 supporting electrolyte.

3.2 Electrochemical investigation of monomers and electropolymerization

The monomers show clearly different electrochemical properties both in terms of oxidation and reduction (**Figure 2,3**). **1** due to the D-D-D structure undergoes only oxidation, no reduction was observed within the electrochemical potential window. The oxidation comprises two reversible signals that can be attributed to the first and second oxidation steps of phenothiazine. The first oxidation process clearly leads to formation of a stable radical cation located at phenothiazine (see EPR section). Second redox couple should therefore be associated with the formation of a dication. The following oxidation processes can be associated with oxidation of carbazole moieties. This reaction is irreversible and leads to formation of a conductive polymer. The compound **2** oxidizes solely at the carbazole moieties, which results in formation of a polymer, similarly to **1**. This compound however, due to the D-A-D structure, also undergoes reduction. A reduction peak (see **Figure 2**) can be observed within the electrochemical window, moreover the process is reversible. Further

investigation of the reduction process by EPR spectroscopy confirms the formation of a stable radical anion located at the acridone moiety in this case. Carbazole moieties in **2** oxidize at lower potential than in **1**, but **1** contains an electron-rich and **2** bears electron-deficient core. This happens due to the fact that oxidation of carbazoles in **1** undergoes with the bicationic ($\mathbf{1}^{2+}$) instead of the neutral form. Such a bication is repulsed from the working electrode surface at positive potential applied, moreover the phenothiazine bication core acts now as an electron-deficient unit. Both effects draw the oxidation potential of carbazole units in **1** to higher values.

As observed with DPV (**Figure 2**) at positive potentials, oxidation of **1** over 1 V potential is complicated, comprising many overlapping peaks. These are the signals of electropolymerization overlapped with the electrochemical response of the forming polymer. On the other hand oxidation of **2** is well resolved, comprising two clearly visible peaks. The first peak has to be associated with the monoelectron oxidation of a single carbazole moiety of **2**, the second process is probably associated with electrochemical response of the forming polymer due to its broadened shape. It is worth to note that the oxidation peak of **2** recorded with CV technique is stretched and deformed, this is because it actually consists of two signals mentioned above (as seen by DPV), that are overlapped.

Figure 2. a), b) Cyclic voltammograms of monomers showing first oxidation / reduction cycles. c), d) Cyclic voltammograms showing electropolymerization process in consecutive scans (black line); Stability of the polymer recorded in monomer-free solution (red line). Oxidation recorded in DCM, reduction in THF solutions of Bu_4NBF_4 supporting electrolyte. Scan rate 0.05 V s^{-1}.

As mentioned previously, the two monomers electropolymerize well, forming a stable polymeric film (see **Figure 3**). The electropolymerization process is induced by the presence of carbazole moieties, that after monoelectron oxidation undergo a coupling reaction. Although carbazole appears to be a bifunctional monomer, recent works [50,51] suggest carbazole acting as a monofunctional moiety in the molecular systems comprising two or more *N*-carbazolyl species. This also seems to be true in the monomers presented here and is supported by (spectro)electrochemical data. In example, the polymers do not increase their conjugation length as presented in the voltammograms – oxidation *onset* remains unchanged in following polymerization scans. Both polymers show electrochemical responses similar to the already reported cases. [52] The first oxidation process of the polymers has to be attributed to formation of polarons, whereas the second to bipolaronic species, which is further confirmed by spectroelectrochemistry.

Figure 3. Cyclic voltammograms of poly(**2**) recorded in DCM and THF solutions of Bu_4NBF_4 supporting electrolyte. Scan rate 0.05 V s^{-1}.

Following the reasoning given above, the proposed polymer structure of poly(**1**) and poly(**2**) is shown in **Scheme 3**. It becomes clear that the acridone/phenothiazine bridge units break the conjugation between bicarbazole bridges, resulting in formation of a polymer with short conjugation length. Please also see **Figure S3-S6**. The calculations performed on idealized trimers show that although there is some conjugation between the bicarbazoles and cores, the units are clearly out of plane. Polymers inherit some features of the monomers, such as redox or optical properties. In particular, the polymer of a D-D-D monomer consequently does not reduce, moreover, the neutral film is colorless, similarly to the solution of the monomer. On the other hand, poly(**2**) color is similar to the yellow color of monomer's solution, due to the presence of a similar charge transfer band, absorbing blue light. Poly(**2**) also shows a

reduction process of *quasi*-reversible character at the potential similar to the redox pair of the monomer (see **Figure 4**). Clearly, the reduction of the polymer involves the acridone species as in both cases: the monomer and polymer the reduction occurs at almost the same potential, -2.07 V and -2.15 V, respectively (see **Table 2**). In this case, due to limited diffusion rate of counter ions the anodic and cathodic peak are stretched and deformed. EPR investigation of the polymer reveals hardly no signal upon reduction of the polymer. This suggests a somehow regular, stacked structure of the polymer, allowing the radical anions of acridone to stack, forming i.e. spinless dimers, which is similar to the already reported dimers in ethylenedioxythiophene-based systems. [9,53]

Scheme 3. Proposed structure of electrodeposited polymers studied in this work.

At this point it is important to note the coincidence of electrochemical and optical energy gap of **2** and poly(**2**). The values are very close in both cases suggesting electron binding energy of zero or almost zero. In this case an error of ± 0.03 eV to the values can be assumed. This is still a debate whether forbidden transition such as n-π* or CT can be used to determine energy gap of a molecule as respective absorption band may not be visible in the spectrum. The answer to this question is not definite, in some cases a forbidden transition has relatively large oscillator strength, thus being well defined in the absorption spectrum. If that condition is met, as in **2** and poly(**2**), the optical energy gap can be determined properly with a small error.

Table 2. Electrochemical properties of investigated molecules.

3.3 UV-Vis-NIR spectroelectrochemical investigation of monomers and polymers

To fully understand the electrochromic response of polymers it is necessary to study the oxidation of monomers first (**Figure 5**). In case of **1** the most interesting part is the oxidation of phenothiazine moiety leading to the formation of a monocation (cation radical) and, at higher potential applied, a bication. Both these species are seen in the absorption spectra. Interestingly, the absorption of a phenothiazine cation radical is very specific and clearly is not present in the spectra of oxidized polymer. Oxidation of **2** leads to formation of a polymer which is a result of coupling of cation radicals originating from carbazole moieties. Due to the similarity of monomer's and polymer's cation radical structure the spectra observed resemble the electrochromic response of poly(**2**).

Figure 4. a), b) UV-Vis-NIR spectroelectrochemical analysis of electrochemical oxidation of **1** and **2**; c), d) Electrochromic response of respective polymers. P1, P2 denote first and second polaronic band; BP bipolaronic band; N neutral polymer absorption bands. Spectra recorded in DCM / 0.1 mol dm^{-3} Bu_4NBF_4 supporting electrolyte solution using ITO coated quartz working electrode.

Electrochromic response of polymers is similar to the already reported [52] cases. Two polaronic bands (P1, P2) are arising in the first oxidation step and one bipolaronic (BP) arises above a specific potential in the second oxidation step. The potentials at which formation of polarons/bipolarons is observed are in good correlation with the *onset* potential of the first and second oxidation peak of polymers, respectively. Therefore figures determining *onset* potential of formation of bipolarons allow to attribute the first redox reaction in polymers to the neutral ↔ polaronic redox process. The second redox process should consequently be attributed to the polaronic ↔ bipolaronic redox process. In both cases oxidation of the polymeric film shows diminishing absorption of the neutral polymer absorption bands (N). This is due to oxidation of bis(carbazolyl) bridges that connect mers. Interestingly, in both

cases there is an isosbestic point clearly visible between N and P1 bands. As no shift of that point is observed, this indicates perfect reversibility of the doping/dedoping process between neutral and polaronic forms. Additional isosbestic point can be observed between P1 and BP bands in poly(**2**). This is rather associated with the presence of a CT band in the polymer, which is discussed below. The presence of an isosbestic point here suggests the process of bipolarons formation to be connected with the diminish of the CT band.

Poly(**2**) similarly to the monomer shows a charge transfer transition. The charge transfer appears clearly between the non-conjugated units of acridone (acceptor) and bicarbazole bridges (donor). Interestingly, the first polaronic band (P1) of the polymer is overlapped with the CT absorption band of a neutral film. The polaronic band grows on the top of the CT band and both bands are still overlapped at the potential of 0.60 V. Above that potential, along with the formation of bipolarons, the CT band diminishes. The band maximum shifts giving eventually absorbtion spectrum which is much more similar to the respective spectrum of poly(**1**) which does not have a CT. That means the polymer in a bipolaronic state shows no CT due to the lack of electrons at HOMO (as for neutral form), so HOMO→LUMO transition (CT) is suppressed.

What is even more interesting is that the electrochromic response of poly(**1**) does not clearly show the involvement of radical cations nor bications of phenothiazine. The polymer behaves on one hand very similar to poly(**2**) showing similar polaronic and bipolaronic bands – on the other hand, due to the absence of the CT band, the film is colorless. Thin films of poly(**1**) are not visible to human eye, but they become visible upon oxidation. This behavior is potentially interesting for applications such as electrochromic tinted windows. Electrochromic response of the polymer is however interesting as no observable evidence for the formation of normal phenothiazine radical cation / bication is present in the absorption spectra. This is further discussed in the ESR spectroelectrochemistry section.

3.4 ESR spectroelectrochemical investigation of monomers and polymers

To evaluate the origin of radical anion/cation species formed in the reversible redox processes the EPR technique has been used. The results comply with intuitive expectations, that reduction of **2** involves the acridone moiety, forming a radical anion, whereas the first oxidation step of **1** leads to production of radical cations localized at the phenothiazine moiety. The EPR spectrum of **2** radical anion shows hyperfine coupling constants of α_{1H} = 0.390 mT (2H) and α_{2H} = 0.365 mT (2H). The observed signal correlates with the simulated spin density for the anion radical (**Figure 6**). Radical is situated the most on atoms of C=O group which also stabilizes the negative charge due to its electron-defficient nature. The observed coupling constants are however only due to delocalization of the spin density over the π-conjugated carbon backbone, no coupling with nitrogen atom (^{14}N, S = 1) is observed as spin density at this atom is negligible. Long range coupling with neighboring atoms is not observed due to a small value of respective coupling constants.

Figure 5. Electron spin resonance (ESR) spectra of investigated cation radicals, linewidth 0.1 mT; hyperfine coupling constants (mT) attributed to the position of coupled nucleus (insets). Hyperfine constants determining coupling with protons are shown at the position of a respective proton, whereas hydrogen atoms themselves are not shown.

On the other hand the **1** radical cation has a spectrum showing hyperfine constants of α_{1N} = 0.749 mT (1N) and α_{1H} = 0.384 mT (2H). This is consistent with the simulated radical spin density (**Figure 6**). The radical is delocalized over the π-conjugated backbone, but the nitrogen and sulfur atoms also contribute to the structure. Coupling constants with nitrogen atoms of carbazolyl units are not observed due to their small values.

Figure 6. Spin density at the B3LYP/6-31G(d,p)/PBF(DCM) for investigated radicals. Isovalue is equal to 0.003.

The polymers however show a rather typical behavior for carbazole polymers, nevertheless this is not an expected behavior when their structure is considered (see **Figure 7**, **8**). Both polymers show no EPR signal in the neutral state suggesting no polaronic species are trapped or remain in defects / at the chain ends. The polymers show a rapid increase of EPR signal intensity upon film oxidation indicating the formation of polaronic species. The response of the polymers is perfectly reversible in the potential window shown. Upon expansion of the potential range to higher potential values the response becomes no longer perfectly reversible as, due to formation of bipolaronic species and long experiment times, the film undergoes slow degradation. The results shown here are therefore limited to the potential range where polymers show fine stability. Signal width decrease along with the decrease of the giromagnetic factor (*g*-factor) observed is an indication of formation of polarons. When the relative spin concentration increases, both factors stabilize their values indicating formation of a narrow variety of polaronic states. This shows that polymers have a regular structure and is consistent with the proposed polymer structure (**Scheme 3**) as the radicals formed localize mostly at bicarbazole bridges in the polymer. Application of a potential of 0.7-0.9 V to the polymer films results in formation of bipolarons. This can be observed as a decrease or plateau of spin concentration. When the polaron concentration reaches a high level the existing or newly formed polarons become further oxidized to bipolarons. The formation of bipolarons is also often connected with slight broadening of the EPR signal that can be observed at higher potentials in poly(**2**) film.

Figure 7. ESR spectroelectrochemical analysis of poly(**1**). a) selected spectra; b) relative spin concentration vs. potential applied; c) signal width vs. potential applied; d) *g*-factor vs. potential applied. A cyclic voltamogram of the polymer film recorded at 0.01 V s^{-1} scan speed prior to the measurement is shown in figures b), c), d). Linewidth 0.05 mT.

The only question that arises in the interpretation of the polymers' behavior is why it is that similar. In case of poly(**1**) normally it would be expected that formation of radical cations occurs not only at bicarbazoles but also at phenothiazine units. The radicals observed in polymers show a g-factor of g = 2.0034-2.0035, which is much lower than the value for cation radical formed by **1**, which is g = 2.0052. If the formation of such phenothiazine-localized radical cations was a fact, there would be observed a large (or at least any) change of the g-factor during the potential sweep (i.e. oxidation of phenothiazine preceding oxidation of bicarbazoles or *vice versa*), however, this does not happen. Moreover, the EPR signal clearly indicates a presence of only one type of radical species (**Figure S7**). Interestingly, the signal of phenothiazine redox couple has not been observed in electrochemistry nor UV-Vis-NIR spectroelectrochemistry. Explanation of this fact is that the geometry of the polymer, especially at oxidized state, allows the phenothiazine to be conjugated with the carbazole moiety. In this situation the formation of a radical coupled with a nitrogen atom ("normal" phenothiazine radical cation) is thus inhibited. As such radical cations are not formed, their characteristical absorption bands cannot be observed in UV-Vis-NIR spectroelectrochemistry of poly(**1**).

Figure 8. ESR spectroelectrochemical analysis of poly(**2**). a) selected spectra; b) relative spin concentration vs. potential applied; c) signal width vs. potential applied; d) *g*-factor vs. potential applied. A cyclic voltamogram of the polymer film recorded at 0.01 V s^{-1} scan speed prior to the measurement is shown in figures b), c), d). Linewidth 0.04 mT.

Due to the conjugation between bicarbazoles and phenothiazine another kind of radical cation and bication species is likely to be formed. Also see Figure **S3**, **S4**. Such as polarons involve only the carbon atoms of phenothiazine, thus chromophoric nitrogen atom of this unit does not play a role. Very similar behavior has already been reported in 2,7-linked chalcogenophene-carbazole polymers [54].

4 Conclusions

Two novel monomers with *N*-linked carbazole species and D-D-D or D-A-D structure are presented. Both polymerize well, giving stable films. Poly(**1**) has shown particularly interesting behavior, giving no electrochemical, nor spectroelectrochemical evidence for formation of phenothiazine-based radical cations nor bications. Such behavior is a result of conjugation between bicarbazole bridges and phenothiazine in the oxidated state resulting in one oxidized form to be produced, rather than two (bicarbazole, phenothiazine) separately. It was observed that poly(**2**) – D-A-D based polymer shows a CT absorption band, similarly to the monomer. Interestingly, the band is present in the polaronic form of the polymer, while disappears in the bipolaronic form.

Transparency and colorlessness of poly(**1**) gives a promising potential application of the polymer in i.e. electrochromic tinted windows, while ambipolarity of poly(**2**) is promising in a potential application as an emitting layer in polymer light emitting diodes.

Acknowledgments

This work is financially supported by Polish National Science Centre, Project No. 2012/05/B/ST5/00745. P. Data acknowledges award no. 04/040/RGJ17/0052 from the Rector of the Silesian University of Technology for research and development achievements.

References

[1] J.H. Cook, H.A. Al-Attar, A.P. Monkman, Effect of PEDOT-PSS resistivity and work function on PLED performance, Org. Electron. 15 (2014) 245–250. doi:10.1016/j.orgel.2013.11.029.

[2] L. Groenendaal, F. Jonas, D. Freitag, H. Pielartzik, J.R. Reynolds, Poly(3,4-ethylenedioxythiophene) and Its Derivatives: Past, Present, and Future, Adv. Mater. 12 (2000) 481–494. doi:10.1002/(SICI)1521-4095(200004)12:7<481::AID-ADMA481>3.0.CO;2-C.

[3] S. Burns, J. MacLeod, T. Trang Do, P. Sonar, S.D. Yambem, Effect of thermal annealing Super Yellow emissive layer on efficiency of OLEDs, Sci. Rep. 7 (2017) 40805. doi:10.1038/srep40805.

[4] J. Santos, J.H. Cook, H.A. Al-Attar, A.P. Monkman, M.R. Bryce, Fluorene co-polymers with high efficiency deep-blue electroluminescence, J. Mater. Chem. C. 3 (2015) 2479–2483. doi:10.1039/c4tc02766c.

[5] V. Jankus, K. Abdullah, G.C. Griffiths, H. Al-Attar, Y. Zheng, M.R. Bryce, A.P. Monkman, The role of exciplex states in phosphorescent OLEDs with poly(vinylcarbazole) (PVK) host, Org. Electron. Physics, Mater. Appl. 20 (2015) 97–102. doi:10.1016/j.orgel.2015.02.002.

[6] H.A. Al Attar, A.P. Monkman, Dopant effect on the charge injection, transport, and device efficiency of an electrophosphorescent polymeric light-emitting device, Adv. Funct. Mater. 16 (2006) 2231–2242. doi:10.1002/adfm.200600035.

[7] P. Data, P. Pander, M. Lapkowski, A. Swist, J. Soloducho, R.R. Reghu, J. V. Grazulevicius, Unusual properties of electropolymerized 2,7- and 3,6- carbazole derivatives, Electrochim. Acta. 128 (2014) 430–438. doi:10.1016/j.electacta.2013.12.108.

[8] P. Data, P. Pander, P. Zassowski, V. Mimaite, K. Karon, M. Lapkowski, J.V. Grazulevicius, P. Slepski, K. Darowicki, Electrochemically Induced Synthesis of Triphenylamine-based Polyhydrazones, Electrochim. Acta. 230 (2017) 10–21. doi:10.1016/j.electacta.2017.01.132.

[9] P. Pander, P. Data, R. Turczyn, M. Lapkowski, A. Swist, J. Soloducho, A.P. Monkman, Synthesis and characterization of chalcogenophene-based monomers with pyridine acceptor unit, Electrochim. Acta. 210 (2016) 773–782. doi:10.1016/j.electacta.2016.05.185.

[10] A. Patra, Y.H. Wijsboom, S.S. Zade, M. Li, Y. Sheynin, G. Leitus, M. Bendikov, Poly(3,4-ethylenedioxyselenophene), J. Am. Chem. Soc. 130(21) (2008) 6734–6736. doi:10.1021/ja8018675.

[11] W. Yang, J. Zhao, C. Cui, Y. Kong, P. Li, Characterization and Electrochemical Synthesize from Selenophene-Substituted Poly(Triphenylamine) as Anodically Materials for Electrochromic Devices, Int. J. Electrochem. Sci. 7 (2012) 7960-7975.

[12] P. Data, R. Motyka, M. Lapkowski, J. Suwinski, A.P. Monkman, Spectroelectrochemical Analysis of Charge Carriers as a Way of Improving Poly(p-phenylene)-Based Electrochromic Windows, J. Phys. Chem. C. 119 (2015) 20188–20200. doi:10.1021/acs.jpcc.5b06846.

[13] T. V Vernitskaya, O.N. Efimov, Polypyrrole: a conducting polymer; its synthesis, properties and applications, Russ. Chem. Rev. 66 (1997) 443–457. doi:10.1070/RC1997v066n05ABEH000261.

[14] B. Alshammary, F.C. Walsh, P. Herrasti, C. Ponce de Leon, Electrodeposited conductive polymers for controlled drug release: polypyrrole, J. Solid State Electrochem. 20 (2016) 839–859. doi:10.1007/s10008-015-2982-9.

[15] K. Krukiewicz, M. Cichy, P. Ruszkowski, R. Turczyn, T. Jarosz, J.K. Zak, M. Lapkowski, B. Bednarczyk-Cwynar, Betulin-loaded PEDOT films for regional chemotherapy, Mater. Sci. Eng. C. 73 (2017) 611–615. doi:10.1016/j.msec.2016.12.115.

[16] D. Svirskis, J. Travas-Sejdic, A. Rodgers, S. Garg, Electrochemically controlled drug delivery based on intrinsically conducting polymers, J. Control. Release. 146 (2010) 6–15. doi:10.1016/j.jconrel.2010.03.023.

[17] A. Stolarczyk, W. Domagala, R. Turczyn, A. Januszkiewicz – Kaleniak, K. Kempska, K. Krukiewicz, M. Gnus, M. Lapkowski, The influence of oxygen conditioning effect on the permeation properties of polyaniline membranes, Sep. Sci. Technol. 6395 (2016) 1–8. doi:10.1080/01496395.2016.1171241.

[18] T. Mirfakhrai, J.D.W. Madden, R.H. Baughman, Polymer artificial muscles, Mater. Today. 10 (2007) 30–38. doi:10.1016/S1369-7021(07)70048-2.

[19] https://www.nobelprize.org/nobel_prizes/chemistry/laureates/2000/advanced-chemistryprize2000.pdf [accessed 24.04.2017]

[20] U. Mehmood, A. Al-Ahmed, I.A. Hussein, Review on recent advances in polythiophene based photovoltaic devices, Renew. Sustain. Energy Rev. 57 (2016) 550–561. doi:10.1016/j.rser.2015.12.177.

[21] T. Yamamoto, Molecular assembly and properties of polythiophenes, NPG Asia Mater. 2 (2010) 54–60. doi:10.1038/asiamat.2010.37.

[22] P. Data, P. Zassowski, M. Lapkowski, W. Domagala, S. Krompiec, T. Flak, M. Penkala, A. Swist, J. Soloducho, W. Danikiewicz, Electrochemical and spectroelectrochemical comparison of alternated monomers and their copolymers based on carbazole and thiophene derivatives, Electrochim. Acta. 122 (2014) 118–129. doi:10.1016/j.electacta.2013.11.167.

[23] P. Ledwon, S. Pluczyk, K.R. Idzik, R. Beckert, M. Lapkowski, Bipolar properties of polythiophene derivatives with 1,3,5-triazineunits, Electrochim. Acta. 109 (2013) 395–402. doi:10.1016/j.electacta.2013.07.171.

[24] P. Zassowski, S. Golba, L. Skorka, G. Szafraniec-Gorol, M. Matussek, D. Zych, W. Danikiewicz, S. Krompiec, M. Lapkowski, A. Slodek, W. Domagala, Spectroelectrochemistry of alternating ambipolar copolymers of 4,4′- and 2,2′-bipyridine isomers and quaterthiophene, Electrochim. Acta. 231 (2017). doi:http://dx.doi.org/10.1016/j.electacta.2017.01.076.

[25] A. Patra, M. Bendikov, Polyselenophenes, J. Mater. Chem. 20 (2010) 422–433. doi:10.1039/B908983G.

[26] A.A. Jahnke, D.S. Seferos, Polytellurophenes, Macromol. Rapid Commun. 32 (2011) 943–951. doi:10.1002/marc.201100151.

[27] J. Razzell-Hollis, F. Fleischli, A.A. Jahnke, N. Stingelin, D.S. Seferos, J.-S. Kim, Effects of Side-Chain Length and Shape on Polytellurophene Molecular Order and Blend Morphology, J. Phys. Chem. C. 121 (2017) 2088–2098. doi:10.1021/acs.jpcc.6b11675.

[28] A. Patra, V. Agrawal, R. Bhargav, Shahjad, D. Bhardwaj, S. Chand, Y. Sheynin, M. Bendikov, Metal Free Conducting PEDOS, PEDOT, and Their Analogues via an

Unusual Bromine-Catalyzed Polymerization, Macromolecules. 48 (2015) 8760–8764. doi:10.1021/acs.macromol.5b01777.

[29] M. Lapkowski, R. Motyka, J. Suwinski, P. Data, Photoluminescent polytellurophene derivatives of conjugated polymers as a new perspective for molecular electronics, Macromol. Chem. Phys. 213 (2012) 29–35. doi:10.1002/macp.201100384.

[30] P. Data, M. Lapkowski, R. Motyka, J. Suwinski, Electrochemistry and spectroelectrochemistry of a novel selenophene-based monomer, Electrochim. Acta. 59 (2012) 567–572. doi:10.1016/j.electacta.2011.11.021.

[31] M. Ates, N. Uludag, Carbazole derivative synthesis and their electropolymerization, J. Solid State Electrochem. 20 (2016) 2599–2612. doi:10.1007/s10008-016-3269-5.

[32] K. Karon, M. Lapkowski, A. Dabuliene, A. Tomkeviciene, N. Kostiv, J. V. Grazulevicius, Spectroelectrochemical characterization of conducting polymers from star-shaped carbazole-triphenylamine compounds, Electrochim. Acta. 154 (2015) 119–127. doi:10.1016/j.electacta.2014.12.092.

[33] R.R. Reghu, D. Volyniuk, N. Kostiv, K. Norvaisa, J. V. Grazulevicius, Symmetry versus asymmetry: Synthesis and studies of benzotriindole-derived carbazoles displaying different electrochemical and optical properties, Dye. Pigment. 125 (2016) 159–168. doi:10.1016/j.dyepig.2015.10.013.

[34] K. Laba, P. Data, P. Zassowski, K. Karon, M. Lapkowski, P. Wagner, D.L. Officer, G.G. Wallace, Electrochemically induced synthesis of poly(2,6-carbazole), Macromol. Rapid Commun. 36 (2015) 1749–1755. doi:10.1002/marc.201500260.

[35] I. Lévesque, P.-O. Bertrand, N. Blouin, M. Leclerc, S. Zecchin, G. Zotti, C.I. Ratcliffe, D.D. Klug, X. Gao, F. Gao, J.S. Tse, Synthesis and Thermoelectric Properties of Polycarbazole, Polyindolocarbazole, and Polydiindolocarbazole Derivatives, Chem. Mater. 19 (2007) 2128–2138. doi:10.1021/cm070063h.

[36] A. Palma-Cando, U. Scherf, Electrochemically Generated Thin Films of Microporous Polymer Networks: Synthesis, Properties, and Applications, Macromol. Chem. Phys. 217 (2016) 827–841. doi:10.1002/macp.201500484.

[37] F.B. Dias, K.N. Bourdakos, V. Jankus, K.C. Moss, K.T. Kamtekar, V. Bhalla, J. Santos, M.R. Bryce, A.P. Monkman, Triplet harvesting with 100% efficiency by way of thermally activated delayed fluorescence in charge transfer OLED emitters, Adv. Mater. 25 (2013) 3707–3714. doi:10.1002/adma.201300753.

[38] P. Data, P. Pander, M. Okazaki, Y. Takeda, S. Minakata, A.P. Monkman, Dibenzo[a,j]phenazine-Cored Donor-Acceptor-Donor Compounds as Green-to-Red/NIR Thermally Activated Delayed Fluorescence Organic Light Emitters, Angew. Chemie - Int. Ed. 55 (2016) 5739–5744. doi:10.1002/anie.201600113.

[39] H. Uoyama, K. Goushi, K. Shizu, H. Nomura, C. Adachi, Highly efficient organic light-emitting diodes from delayed fluorescence., Nature. 492 (2012) 234–8. doi:10.1038/nature11687.

[40] L. Mei, J. Hu, X. Cao, F. Wang, C. Zheng, Y. Tao, X. Zhang, W. Huang, The inductive-effect of electron withdrawing trifluoromethyl for thermally activated delayed fluorescence: tunable emission from tetra- to penta-carbazole in solution processed blue OLEDs., Chem. Commun. 51 (2015) 13024–7. doi:10.1039/c5cc04126k.

[41] F.B. Dias, T.J. Penfold, A.P. Monkman, Photophysics of thermally activated delayed fluorescence molecules, Methods Appl. Fluoresc. 5 (2017) 12001. doi:10.1088/2050-6120/aa537e.

[42] Z. Xi, F. Liu, Y. Zhou, W. Chen, CuI/L (L=pyridine-functionalized 1,3-diketones) catalyzed C-N coupling reactions of aryl halides with NH-containing heterocycles, Tetrahedron 64 (2008) 4254-4259.

[43] H.-S. Kim, E.-S. Yu, Y.-H. Kim, J.-H. Kim, Compound for organic photoelectric device and organic photoelectric device including the same, US 2012/0305900 A1.

[44] J. Doskocz, J. Soloducho, J. Cabaj, M. Lapkowski, S. Golba, K. Palewska, Development in synthesis, electrochemistry, LB moieties of phenothiazine based units, Electroanalysis 19 (2007) 1394-1401.

[45] A. Swist, J. Cabaj, J. Soloducho, P. Data, M. Lapkowski, Novel acridone-based branched blocks as highly fluorescent materials, Synth. Met. 180 (2013) 1-8. doi: 10.1016/j.synthmet.2013.07.020.

[46] A.D. Bochevarov, E. Harder, T.F. Hughes, J.R. Greenwood, D.A. Braden, D.M. Philipp, D. Rinaldo, M.D. Halls, J. Zhang, R.A. Friesner, Jaguar: A high-performance quantum chemistry software program with strengths in life and materials sciences, Int. J. Quantum Chem. 113 (2013) 2110–2142. doi:10.1002/qua.24481.

[47] Materials Science Suite 2016-3, Schrödinger, LLC, New York, NY, 2016.

[48] M.C. Castex, C. Olivero, G. Pichler, D. Adès, A. Siove, Fluorescence, room temperature phosphorescence and photodegradation of carbazole compounds in

irradiated poly(methyl methacrylate) matrices, Synth. Met. 156 (2006) 699–704. doi:10.1016/j.synthmet.2006.03.015.

[49] B.K. Sharma, A.M. Shaikh, N. Agarwal, R.M. Kamble, Synthesis, photophysical and electrochemical studies of acridone-amine based donor–acceptors for hole transport materials, RSC Adv. 6 (2016) 17129–17137. doi:10.1039/C5RA25115J.

[50] K. Karon, M. Lapkowski, G. Juozas, Electrochemical and UV-Vis/ESR spectroelectrochemical properties of polymers obtained from isomeric 2,7- and 3,6-linked carbazole trimers; Influence of the linking topology on polymers properties, Electrochim. Acta. 123 (2014) 176–182. doi:10.1016/j.electacta.2013.12.180.

[51] M. Lapkowski, J. Zak, K. Karon, B. Marciniec, W. Prukala, The mixed carbon-nitrogen conjugation in the carbazole based polymer; The electrochemical, UVVis, EPR, and IR studies on 1,4 bis[(E)2-(9H-carbazol-9-yl) vinyl]benzene, Electrochim. Acta. 56 (2011) 4105–4111. doi:10.1016/j.electacta.2011.01.114.

[52] A. Brzeczek, P. Ledwon, P. Data, P. Zassowski, S. Golba, K. Walczak, M. Lapkowski, Synthesis and properties of 1,3,5-tricarbazolylbenzenes with star-shaped architecture, Dye. Pigment. 113 (2015) 640–648. doi:10.1016/j.dyepig.2014.09.033.

[53] P. Data, A. Swist, M. Lapkowski, J. Soloducho, K. Darowicki, A.P. Monkman, Evidence for Solid State Electrochemical Degradation Within a Small Molecule OLED, Electrochim. Acta. 184 (2015) 86–93. doi:10.1016/j.electacta.2015.10.047.

[54] P. Pander, R. Motyka, P. Zassowski, M. Lapkowski, A. Swist, P. Data, Electrochromic Properties of Novel Selenophene and Tellurophene Derivatives Based on Carbazole and Triphenylamine Core, J. Phys. Chem. C, Article ASAP, doi: 10.1021/acs.jpcc.7b00216.

[55] C.M. Cardona, W. Li, A.E. Kaifer, D. Stockdale, G.C. Bazan, Electrochemical considerations for determining absolute frontier orbital energy levels of conjugated polymers for solar cell applications, Adv. Mater. 23 (2011) 2367–2371. doi:10.1002/adma.201004554.

[56] J.-L. Bredas, Mind the gap!, Mater. Horiz. 1 (2014) 17–19. doi:10.1039/C3MH00098B.

Figure 1

Click here to download high resolution image

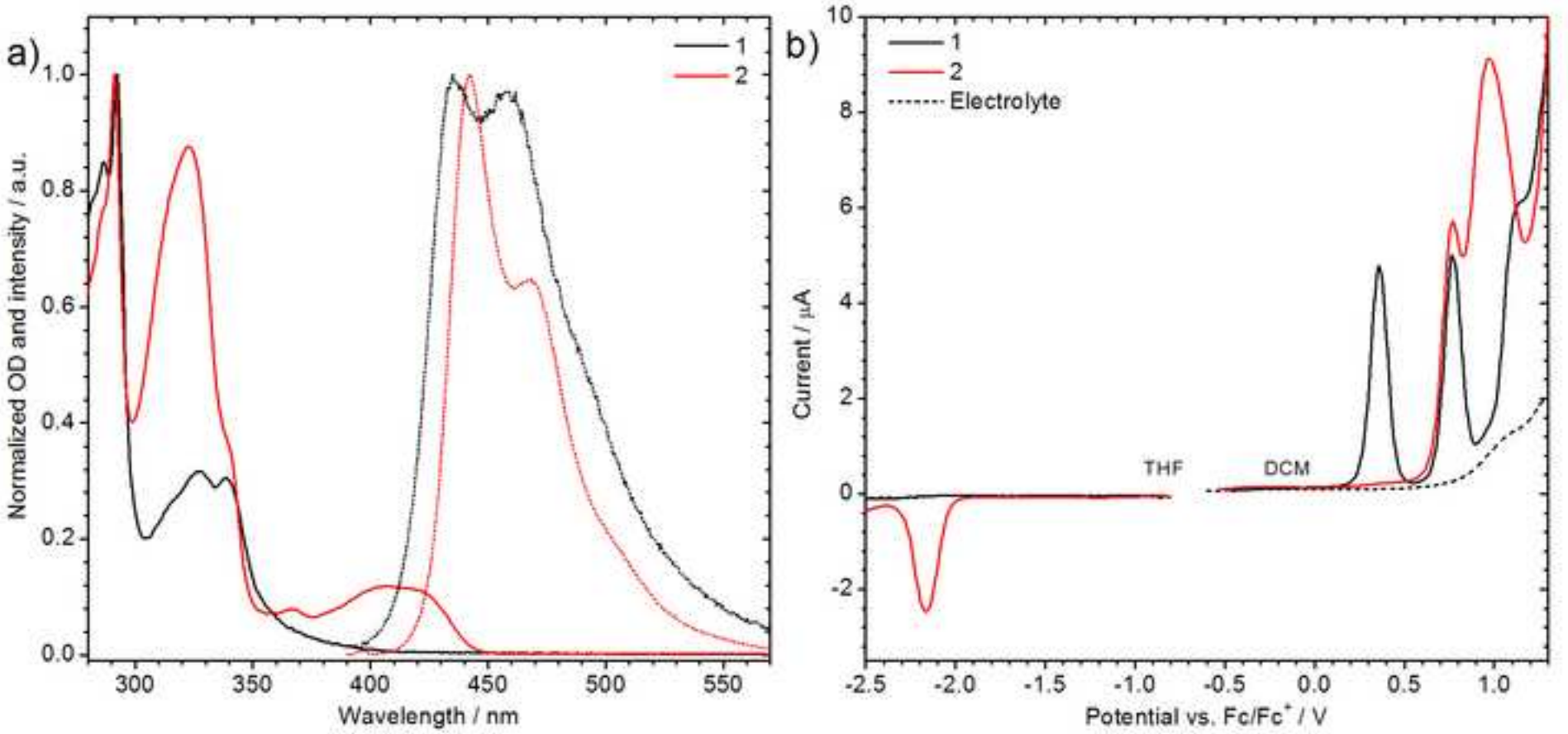

Figure 2

Click here to download high resolution image

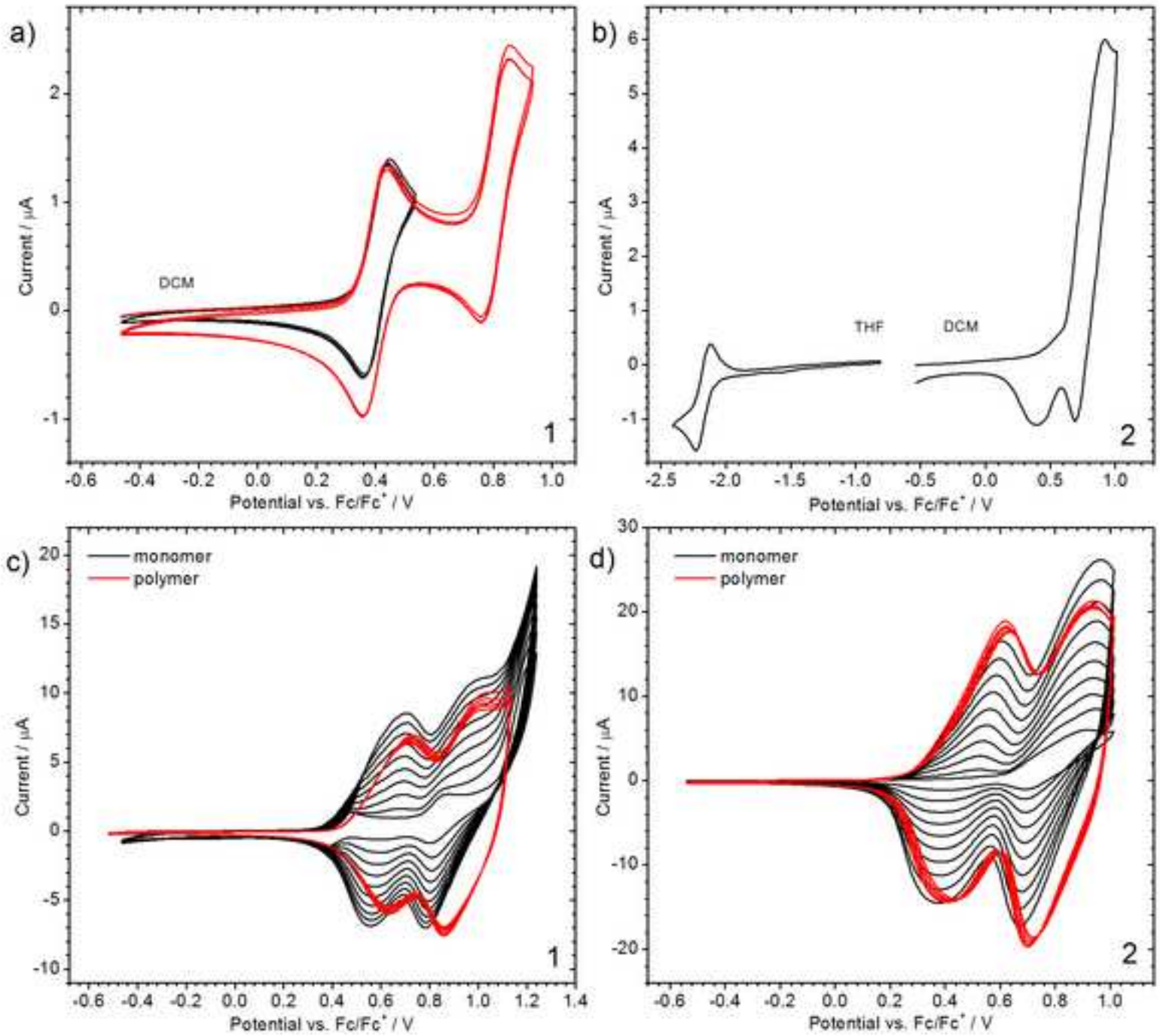

Figure 3

Click here to download high resolution image

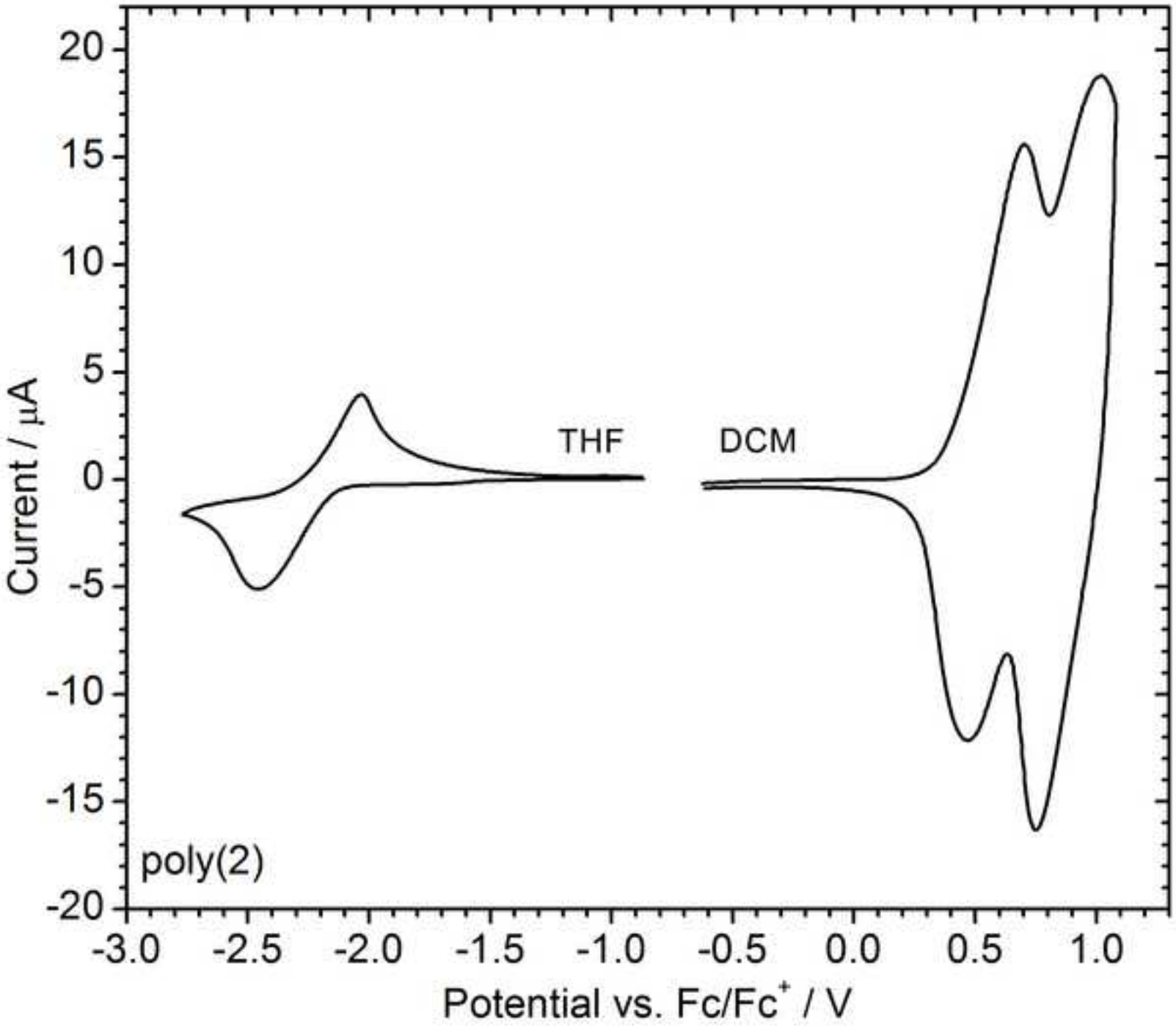

Figure 4

Click here to download high resolution image

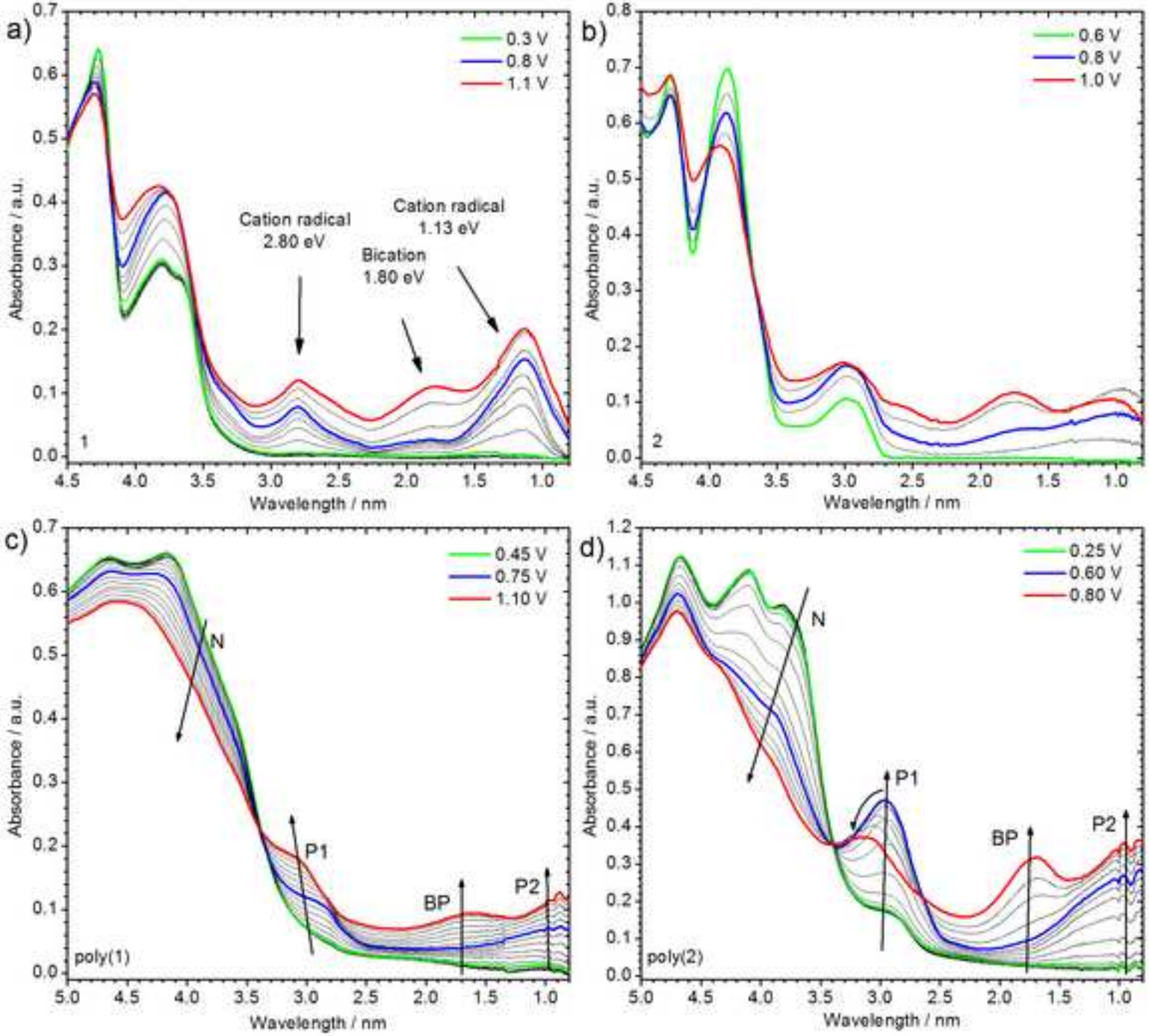

Figure 5

Click here to download high resolution image

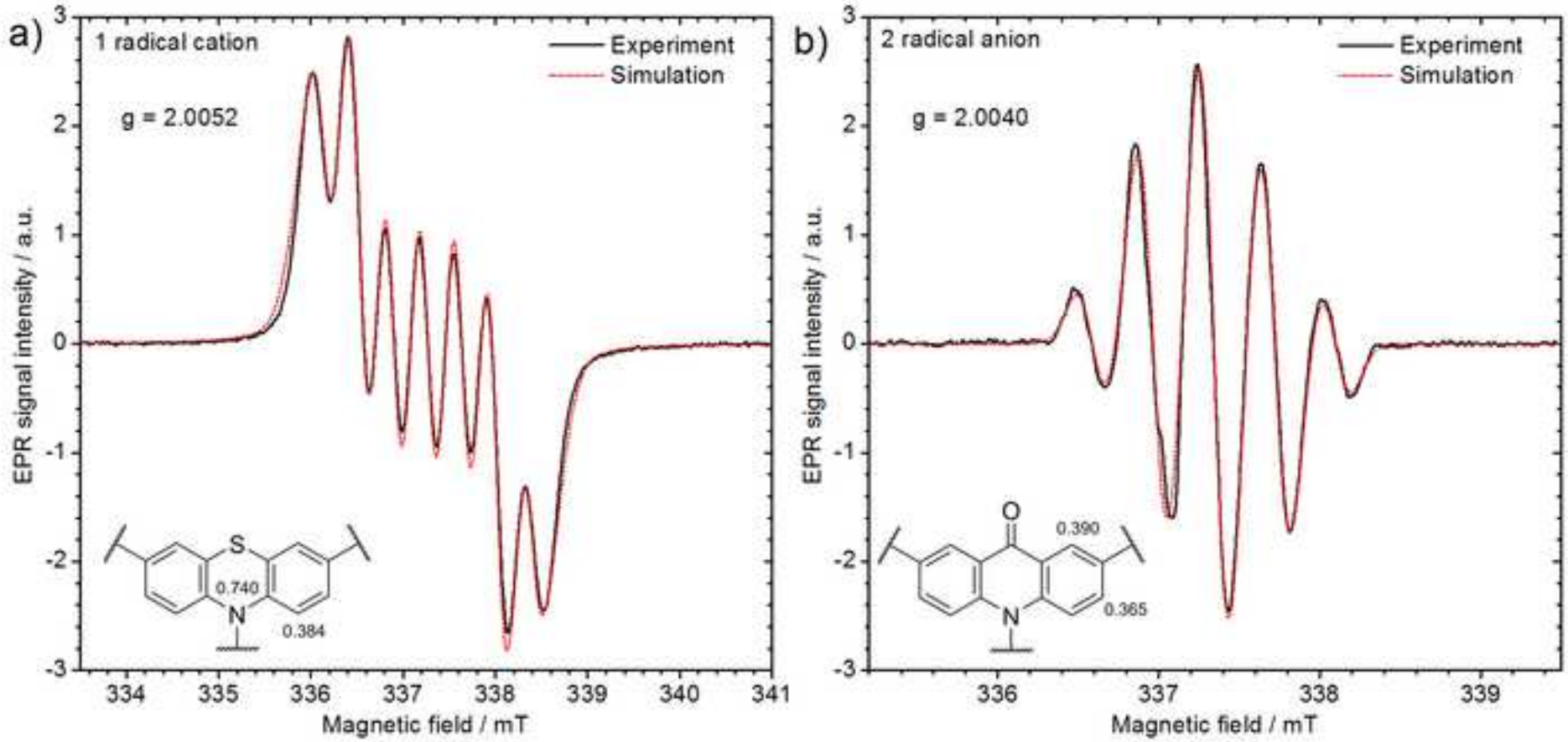

Figure 6

Click here to download high resolution image

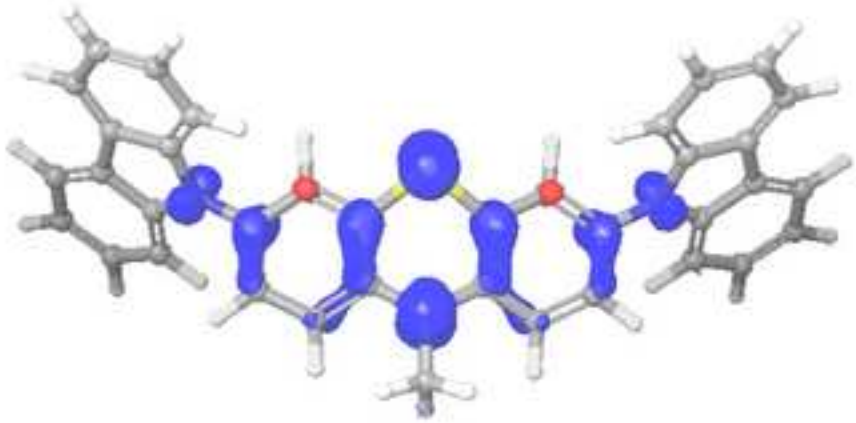

1 radical cation

2 radical anion

Figure 7

Click here to download high resolution image

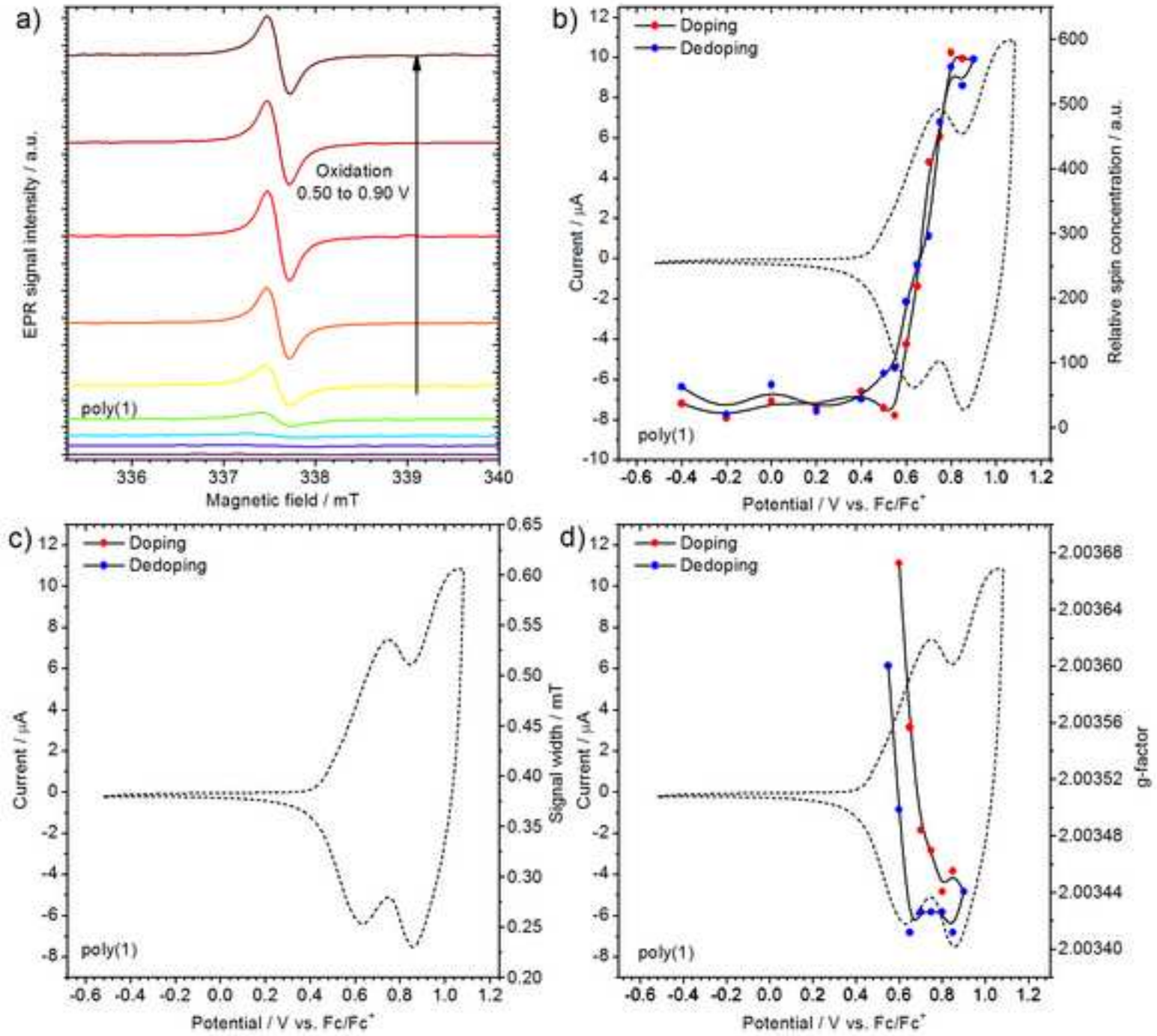

Figure 8

Click here to download high resolution image

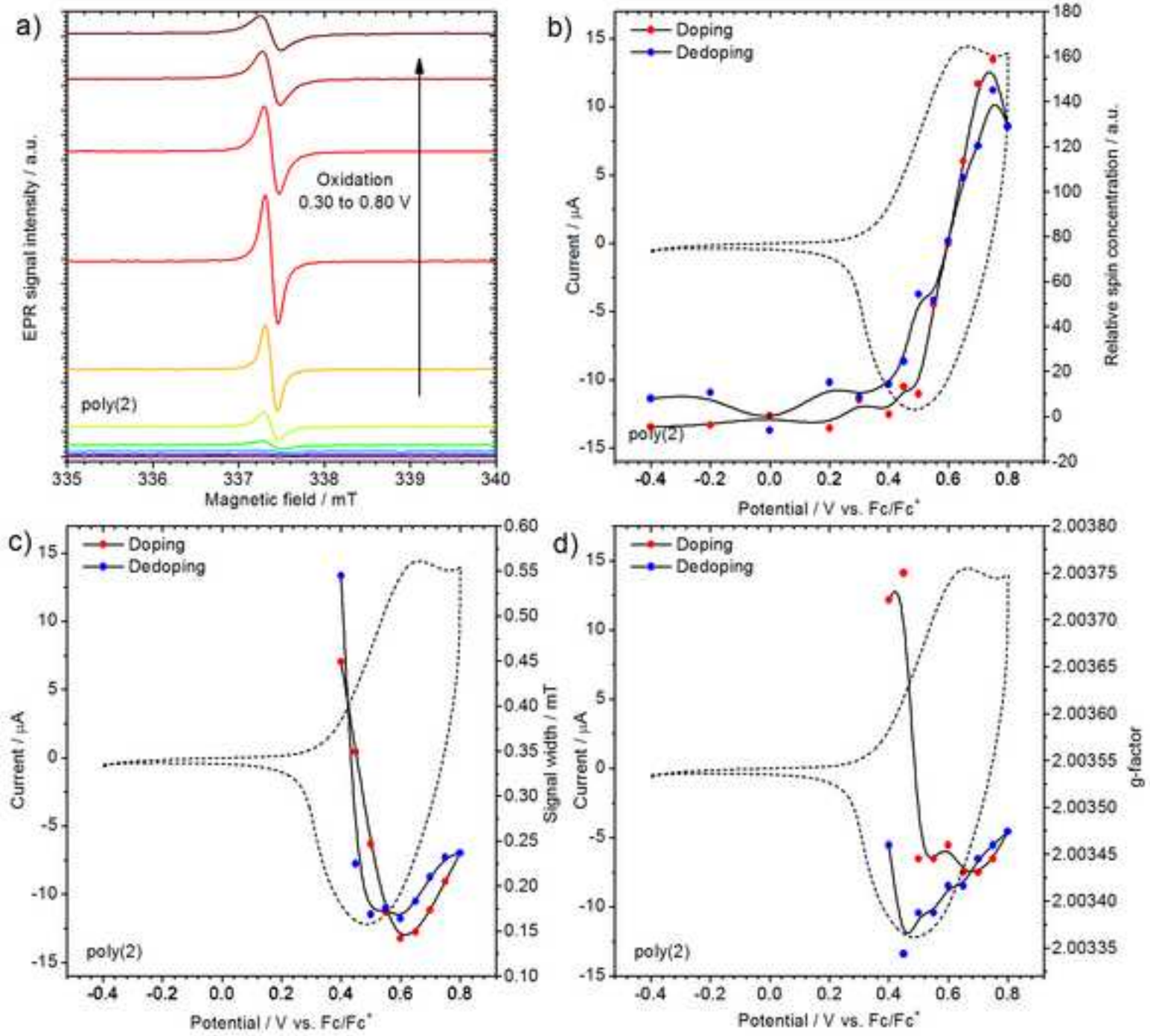

Scheme 1

Click here to download high resolution image

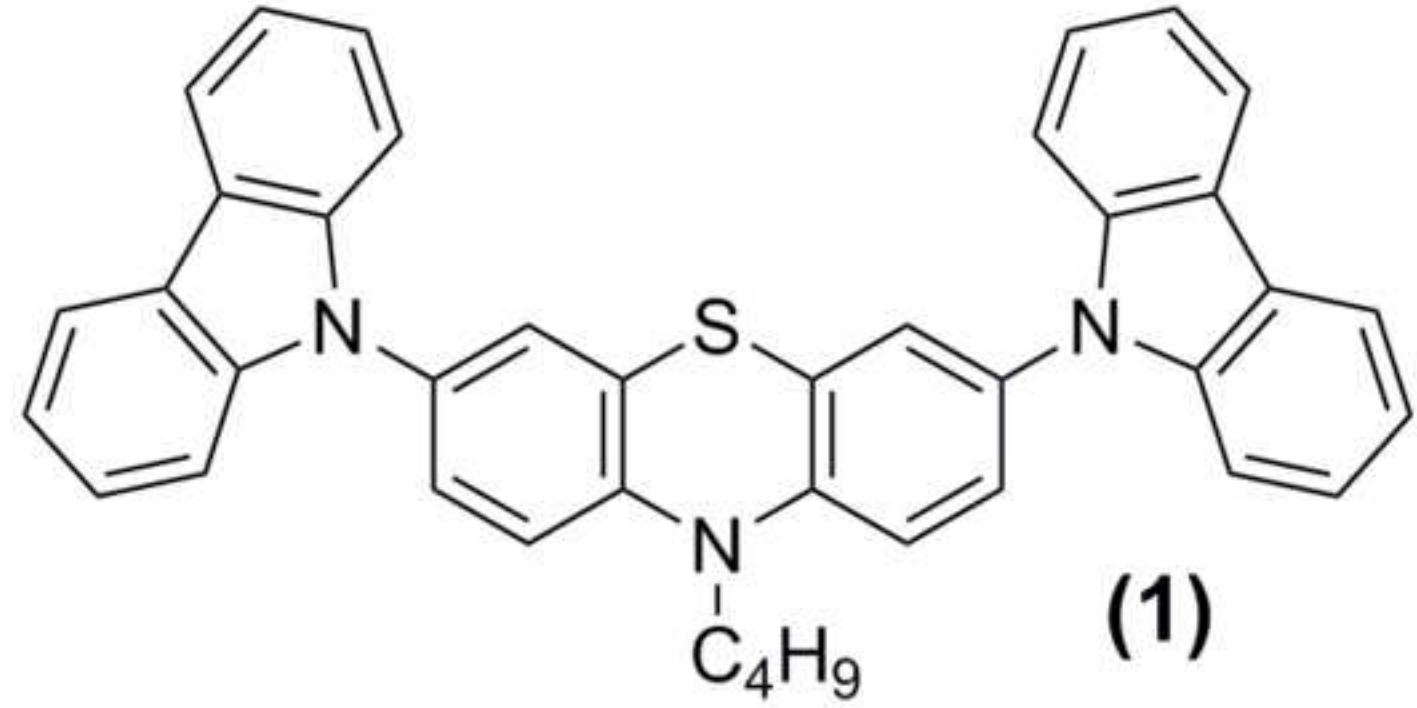

(1)

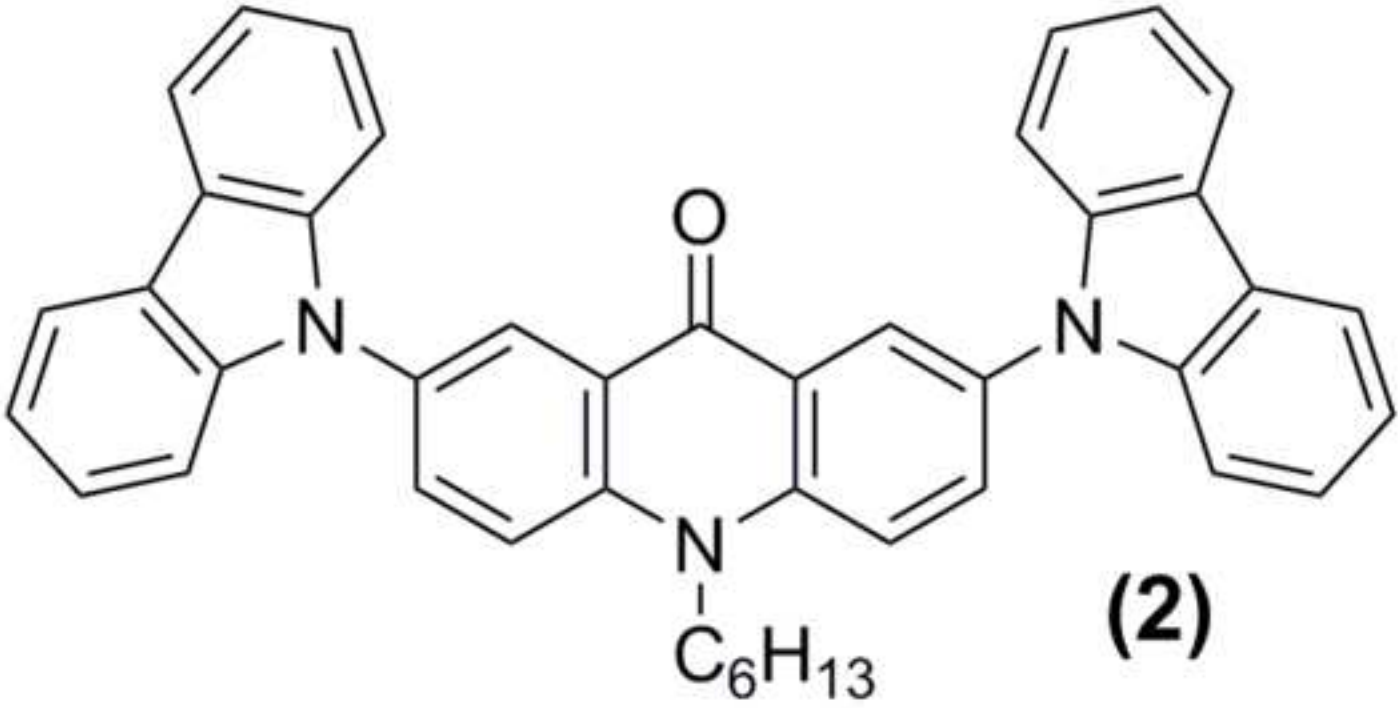

(2)

Scheme 2

Click here to download high resolution image

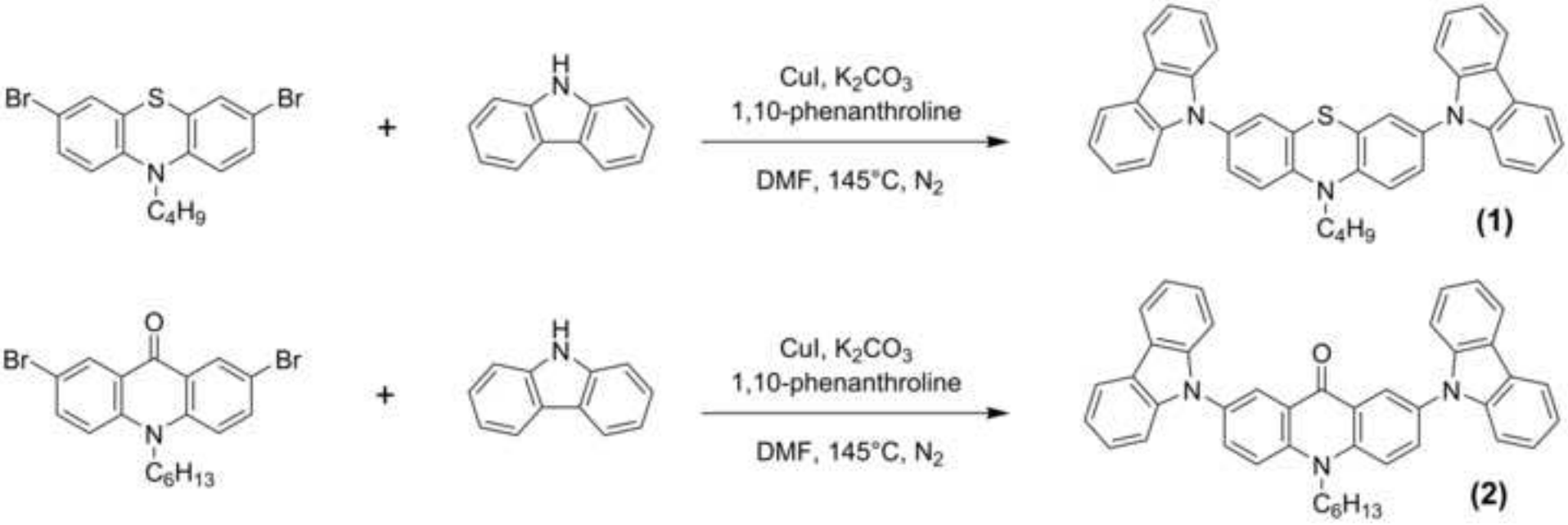

Scheme 3

Click here to download high resolution image

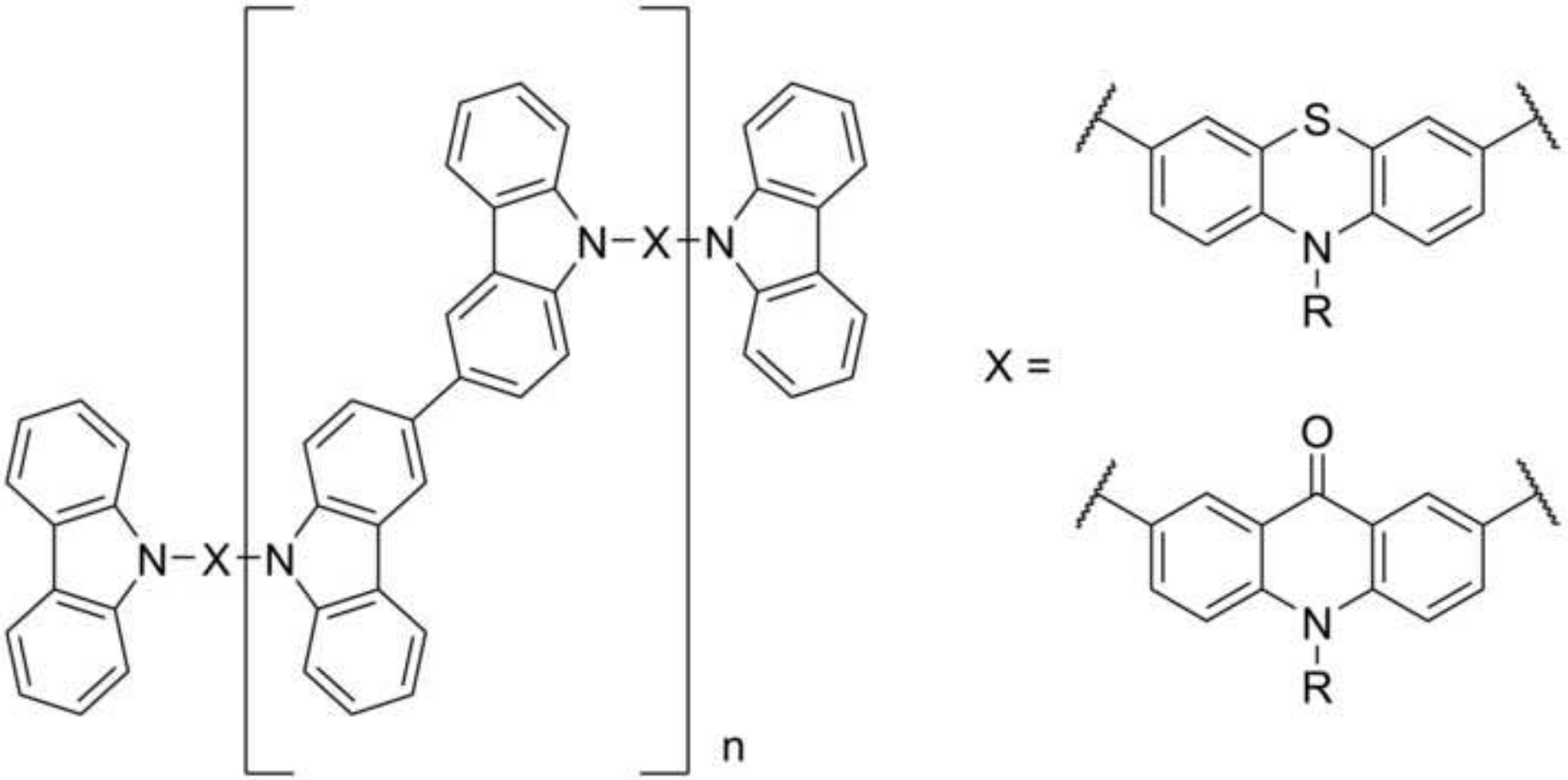

Table 1

Compound	λ_{abs}, nm [a]	λ_{em}, nm [b]	Φ_{PL} [c]
1	293, 327, 339	436, 458	0.56
2	293, 323, 409	442, 467	0.04

[a] Absorption maxima; [b] Emission maxima; [c] Photoluminescence quantum yield recorded in degassed solution against diphenylanthracene Φ_{PL}=0.9 in degassed cyclohexane. Note all data recorded in methylcyclohexane.

Table 2

Compound / polymer	E_{ox}^{onset}, V[a]	E_{red}^{onset}, V[b]	IP, eV[c]	EA, eV[d]	E_g^{el}, eV[e]	E_g^{opt}, eV[f]
1	0.34	-	5.44	2.32*	-	3.12
Poly(1)	0.51	-	5.61	2.62*	-	2.99
2	0.69	-2.07	5.79	3.03	2.75	2.72
Poly(2)	0.39	-2.15	5.49	2.95	2.54	2.57

[a] *Onset* oxidation potential; [b] *Onset* reduction potential; [c] Ionization potential IP = |e| (E_{ox}^{onset} + 5.1); [d] [55,56] Electron affinity EA = |e| (E_{red}^{onset} + 5.1); [55,56] [e] Electrochemical energy gap E_g^{el} = |e| (E_{ox}^{onset} - E_{red}^{onset}); [55,56] [f] Optical band gap E_g^{opt} = 1240/λ_{onset} (eV), where λ_{onset} (nm) is absorption onset of monomer solution or polymer film in DCM. Please note the equation is derived as a practical form of expression E_g^{opt} = hc/λ_{onset} , where h – Planck's constant, c – speed of light; * EA estimated using optical energy gap EA = IP - E_g^{opt}. Electrochemical potentials given are relative to ferrocene/ferricinium (Fc/Fc^+) redox couple.

Supplementary Materials

Click here to download Supplementary Materials: Manuscript elacta SI.doc